3-23-2016

Image-Based 3D Morphometric Analysis of the Clavicle Intramedullary (IM) Canal

Jazmine Aira

Image-Based 3D Morphometric Analysis of the Clavicle Intramedullary (IM) Canal

by

Jazmine Aira

A thesis submitted in partial fulfillment
of the requirements for the degree of
Master of Science in Biomedical Engineering
Department of Chemical and Biomedical Engineering
College of Engineering
University of South Florida

Co-Major Professor: William E. Lee III, Ph.D.
Co-Major Professor: Peter Simon, Ph.D.
Stephanie Carey, Ph.D.

Date of Approval:
March 11, 2016

Keywords: Bone Geometry, Computerized Tomography (CT) Scan Study, Sexual Dimorphism, Laterality, Endomedullary Devices

DEDICATION

I dedicate this work to my family and friends for their endless patience, love, and support.

ACKNOWLEDGMENTS

Firstly, I would like to express my sincere gratitude to my mentor Dr. Peter Simon for providing me with guidance, knowledge and the motivation I needed to succeed. I also appreciate and thank Dr. William Lee and Dr. Stephanie Carey for their valuable advice and guidance thought my thesis.

I would also like to thank Dr. Mark Frankle for his insight and help in understanding shoulder pathology and the clinical significance of my research. Additional thanks to the researchers at the Foundation for Orthopaedic Research and Education, especially, Dr. Brandon Santoni for allowing me to participate and learn in his lab, and Dr. Sergio Gutierrez for his collaboration in this study.

TABLE OF CONTENTS

LIST OF TABLES

LIST OF FIGURES

ABSTRACT

Midshaft clavicle fractures are very common. Current treatment of choice involves internal fixation with superior or anterior clavicle plating, however their clinical success and patient satisfaction are slowly decreasing. The design of intramedullary (IM) devices is on the rise, but data describing the IM canal parameters is lacking. The aim of this study is to quantify morphometry of the clavicle and its IM canal, and to evaluate the effect of gender and anatomical side. This study used 3-dimensional (3D) image-based models with novel and automated methods of standardization, normalization and bone cross-section evaluation. The data obtained in this thesis presents IM canal and clavicle radius and center deviation parameterized as a function of clavicle length, in addition, its radius of curvature and true length. Results showed that right-sided clavicles tended to be shorter and thicker than left-sided, but only males showed a statistically significant difference in size compared to females ($p<.0001$). The smallest IM canal and clavicle radii were seen at different clavicle lengths (54% and 49%), suggesting that the narrowest region of IM canal cannot be appreciated based on external visualization of the clavicle alone. The narrowing of the IM canal is of special interest because this a potential limiting region for IM device design. Furthermore, the location and value of maximum lateral curvature displacement is different in the IM canal, implying there exists an eccentricity of the IM canal center with respect to the clavicle center.

CHAPTER 1: INTRODUCTION

1.1 Study Motivation

Clavicle fractures are very common; they represent 2-5% of all fractures. Predominately seen in the young adult male population [1], they are typically caused by traumatic events such as motor vehicle collisions (46%), and falls (33%), and sports injuries (7.3%) [2]. The most common site (82%) for fracture is the middle third of the clavicle [1].

Current treatment for displaced mid-shaft clavicle fractures involves internal fixation with superior or anterior clavicle plating [2]. However, external plating has been associated with post-surgical complications including infection, hardware malfunction, and fracture re-occurrence [3]. In addition, exterior plating is aesthetically problematic, as the underlying hardware can be visualized and palpated from the outer skin surface.

Intramedullary (IM) fixation of mid-shaft clavicle fractures may be a feasible surgical alternative to external plate fixation. Normally, these devices are used for the treatment of fractures in other larger long bones, such as those in the arms and legs [4], but are becoming more popular as many recent studies suggest that IM devices are preferable for treating mid-shaft clavicle fractures [5] [6] [7]. Advancements in implant technology have made effective clavicle IM devices possible, but development can be problematic due to the clavicle's intricate shape and small diameter. Currently, data describing the morphometric parameters of the IM canal is lacking, and a 3-dimensional (3D) analysis of its geometry is necessary to obtain these.

Morphometric studies on the clavicle have been performed but are limited by a few noteworthy shortcomings. The work by Andermahr et al. [8] has been the most cited; they used cadaveric clavicles manually cut to measure IM canal diameter, but did not control for angle, position, or slice thickness, so these measurements were left to the bias of the operator. Mathieu et al. [9] evaluated the IM canal morphometry from clavicle CT scans. However, the methodology reported was not 3D as the measurements were taken on planes produced by the CT scanner. The study by Nousirrat et al. [10] was performed on the external third of the clavicle in a similar fashion. Further, the position of clavicle was not controlled for during scanning that may potentially skew the results. King at al. [11] performed a study on 418 clavicles using CT scans, and reported on IM canal parameters. Once again, the study was not 3D as the measurements were taken on limited numbers of axial (Figure A.1) slices.

There are further studies [12] [13] [14] [15] [16] [17], however, that have performed true 3-dimensional (3D) morphometric analyses on the clavicle, but none have addressed internal measurements involving the IM canal or cortical bone thickness. Prior to introduction clinically, a true 3D morphometric study of the clavicular geometry, especially of the IM canal, is necessary to determine the requisite design features of an IM device that may be used to treat clavicle fractures.

1.2 Study Aims

The aim of this study is to quantify the morphometry of the clavicle and its IM canal, namely, cross-sectional width and center depth as a function of clavicle length. IM canal radius of curvature, and absolute and true lengths of the clavicle will also be measured. Furthermore, these parameters will be examined in relationship to each other. In order to eliminate the

subject-specific bias induced by the operator and to perform a true 3D analysis, only 3D image-based models are to be used. Thus, the analysis will not be limited to the position of the patient during the CT scan, but rather determined by the clavicle's own geometry. All algorithms used are fully automated for evaluating each 3D model, eliminating operator bias at every step of the process after the volumetric clavicle model is generated. The final aim is to evaluate the effect of gender and anatomical side on the morphometric parameters of the human clavicle and IM canal.

CHAPTER 2: HUMAN CLAVICLE BACKGROUND

2.1 Human Clavicle Anatomy and Structure

The clavicle is a long bone, located in the anterior portion of the pectoral girdle on each side of the body, directly above the first rib. It extends horizontally across the superior thorax. The medial end of the clavicle is cone shaped and articulates with the manubrium of the sternum at the clavicular notch. This articulation is the only site that directly attaches the pectoral girdle to the axial skeleton, which allows the arm and scapula to move more freely [18]. The lateral end of the clavicle is horizontally flattened and articulates with the acromion of the scapula, forming the acromioclavicular (AC) joint. This diarthrodial joint is formed by the superior and inferior AC ligaments and AC capsule with a fibrocartilaginous meniscal disc in between. These ligaments provide horizontal stability to the joint, while the coracoclavicular ligaments, formed by the trapezoid and conoid ligaments, attach the coracoid process of the scapula to the distal clavicle and provide vertical stability to the AC joint [19] [18]. The clavicle and its joints can be seen in Figure 1.

The superior surface of the bone which lies just deep to the skin is smooth as it does not have muscle or ligament attachments. On the other hand, the inferior aspect of the clavicle has ridges and grooves that serve as ligament attachment sites [18]. The clavicle bone is composed of mostly compact cortical bone with less dense spongy bone in the inner intramedullary (IM) canal, as the clavicle does not have marrow[18]

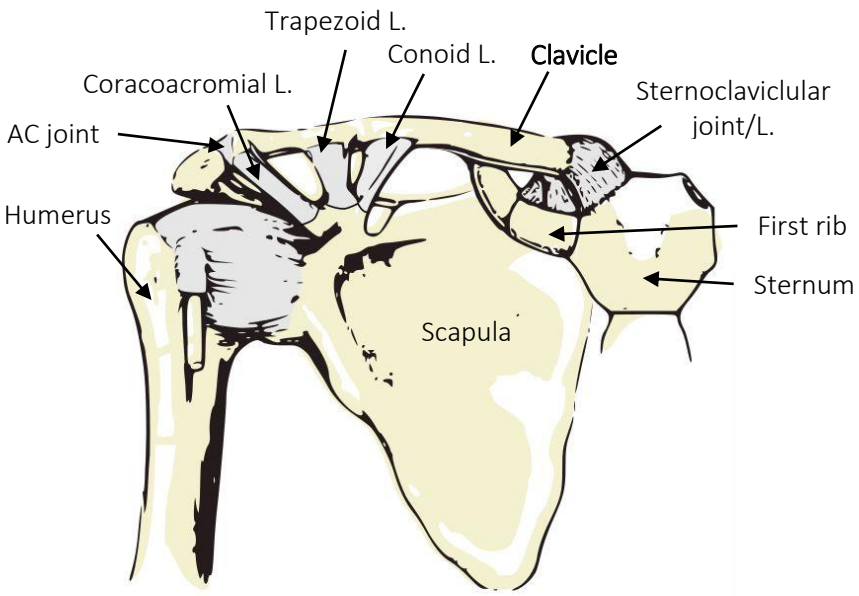

Figure 1 Anatomy of the clavicle and its joints.

In the axial plane, the medial two thirds of clavicle are convex anteriorly, but the lateral third is concave anteriorly, giving the bone its signature S-shape. The clavicle can also be described as having a curvature in the coronal plane, called an inferior/superior curvature [16] (Figure A.2). The middle third of the clavicle shaft is noticeably narrower with a transitional area between the tubular medial end and the flattened lateral end of the clavicle [20]. The large medial curvature of the clavicle passes over and protects several important structures such as the axillary vein and artery, subclavius muscle, and the brachial plexus [18] [21]. The region of weakness of the clavicle, the mid-third, is located just lateral to this curvature, so in the case of a mid-shaft fracture, the underlying structures are likely to be avoided [21].

Long bones are those that are longer than they are wide. With the clavicle being the only exception, all other long bones are formed by endochondral ossification [20]. In this process, the hyaline cartilage “bones” formed during fetal development are replaced with bone tissue. This

occurs as the diaphysis or shaft of the bone grows in length at the epiphyseal plates. However, the clavicle is formed via intramembranous ossification. This process, typically seen in flat bones, starts during fetal development as well, but forms bone tissue from mesenchymal cell differentiation, without the formation of cartilage [18].

Individual clavicle parameters in reference to its anatomy can be seen in Figure A.2. Statistical shape analysis studies of the clavicle have found that, within the same gender and side, clavicle length varies more than the overall shaft diameter among subjects [16]. This finding also applies to the variation in length of the IM canal [22]. As a result of many anatomical studies over the years, the scientific community agrees that men tend to have longer, wider and thicker clavicles with a greater lateral depth (Figure A.2) when compared to women [16].

It is generally accepted that bone mineralization, the deposition of calcium phosphate crystals into the bone matrix, is proportional to the compression forces exerted on that bone [23]. This means that, for example, athletes will typically exhibit denser bones than more inactive individuals. It also has been noted that the bone composition in clavicles of athletes or manual laborers can change, becoming stronger and longer in response to their sensitivity to muscle pull [18]. Variation in bone density has also been observed within the same individuals. Because bone mass will vary depending on its use, upper limb bones exhibit laterality patterns; right-handed individuals are seen with denser right sided radius and ulna, and vice-versa for their left-handed counterparts [24] [25]. However, when it comes to the clavicle, those on the non-dominant side of the body exhibit greater bone densities [25]. In addition, there is no statistical difference between left and right clavicles when looking at degree of surface topography, porosity, and osteophyte formation [26]. Yet, when it comes to age there is a correlation between age and

bone texture, porosity, osteophyte formation and cortex thickness. The older an individual, the more likely it is to observe a degraded bone surface with more/larger pores and osteophytes, while the cortex thickness decreases with age [26].

2.2 Clavicle Function

Besides protecting important underlying structures, the clavicle optimizes arm strength by preserving the correct length-tension relationship of the main muscles that attach to it, thereby increasing the biomechanical lever arms [27]. The sternocleidomastoid muscle has an origin at the medial end of the clavicle; the muscle can elevate the clavicle, aiding in forced inhalation. The trapezius muscle also elevates the clavicle, but it inserts into the clavicle in the lateral end [18]. Along with the weight of the arm, the deltoid and pectoralis major muscles pull the clavicle downward [18] [27].

The clavicle also prevents the scapula and arm from collapsing into the thorax by acting as a strut; thus, it resists horizontal compression along its length. This function is evidenced by the displacement pattern of bones during mid-shaft clavicle fractures; the clavicle is shortened and the shoulder advances medially, called clavicle shortening [18]. Shoulder kinematic studies have also found that the clavicle is an important element in scapula external rotation, upward rotation and posterior tilting [28].

Besides enduring horizontal compression forces when the body is at rest in a neutral position, the clavicle transmits forces from the arms to the axial skeleton when the arms are exerting force on an object. Such forces are seen when the body is pushing a heavy object with arms extended forward or when someone falls forward and extends the arms to break the fall [18].

2.3 Pathology and Clinical Significance

Acromioclavicular (AC) dislocations are injuries to the AC joint involving the capsule, AC ligament and coracoclavicular ligament. They are caused by either direct trauma to the AC region of the shoulder, or by falls where forces are transmitted through the upper extremity. There is a wide range of treatment options for AC dislocations, depending on the severity of injury. While surgery may be advisable for severe injuries, treatment for intermediate separation is still highly debated whether non-operative management is favorable [29].

Even more common than dislocations, is osteoarthritis of the AC joint. Degeneration of this joint can occur from age related wear and tear of the articular disk, posttraumatic or inflammatory arthropathy, clavicle osteolysis, or joint instability. It is thought that repetitive microtrauma to the AC joint can lead to degeneration, a similar mechanism to osteolysis [30].

Distal Clavicle Osteolysis (DCO) is the pathologic resorption of distal clavicle bone matrix. It can occur in traumatic and non-traumatic settings of the shoulder. The most widely accepted etiology is repetitive microtrauma to the distal clavicle causing subchondral stress fractures and bone remodeling. This theory is corroborated by studies that have shown an increased osteoclast activity in osteolytic clavicles along with degenerative articular cartilage, suggesting an active repair process of the joint. DCO has also been diagnosed in patients who partake in regular weight lifting, where the shoulder is hyperextended and the AC joint is under excessive traction during the eccentric phase of bench presses, for example [19].

2.4 Clavicular Fractures

A bone fracture is when the continuity of bone tissue is damaged. Clavicle fractures are very common: 2.6 - 5% of all fractures occur at the clavicle. 68% of those fractures occur in men, and within the male population, the left side is involved 61% of the time [1]

Clavicle fractures can be classified into 3 types based on the location of the clavicle: middle, lateral and medial thirds. Furthermore, these groups can be subcategorized by the complexity of the fracture. The most common region of fracture, the middle third of the shaft, accounts for 81% of all clavicular fractures (Figure 2). This is followed by lateral fractures (17%) and medial fractures (2%). Clavicle fractures, regardless of type, tend to decrease with age except for in male adolescents and male children. Within mid-shaft fractures, 48% of them are displaced, and 19% of them are comminuted, meaning broken into 3 or more fragments. Also, males are more likely to have displaced mid-shaft fractures than females. In children aged 10 or less, the most common type is non-displaced mid-shaft clavicle fractures. With increasing age mid-shaft fractures are still the most frequently observed type, but become less numerous and more frequently displaced [1].

The most common cause of clavicle fracture is traffic accidents (47.5%). This is followed by accidental falls at 33.0%, and sport-related injuries at 7.3% [1]. Forces greater than the critical buckling load of the clavicle can cause mid-shaft clavicle fractures. When an individual falls forward with the arms stretched out to break the fall, impact forces on the hands are transmitted through the arms to the clavicle, causing fractures. Nonetheless, because forces are only indirectly applied to the clavicle, this mechanism is less common and only accounts for 2-5% of all mid-shaft clavicle fractures. Increasing amount of data nowadays suggests that direct blows

to the shoulder region are the most common cause of clavicle fracture; this is explained by the bone's superficial position without protection from muscles.

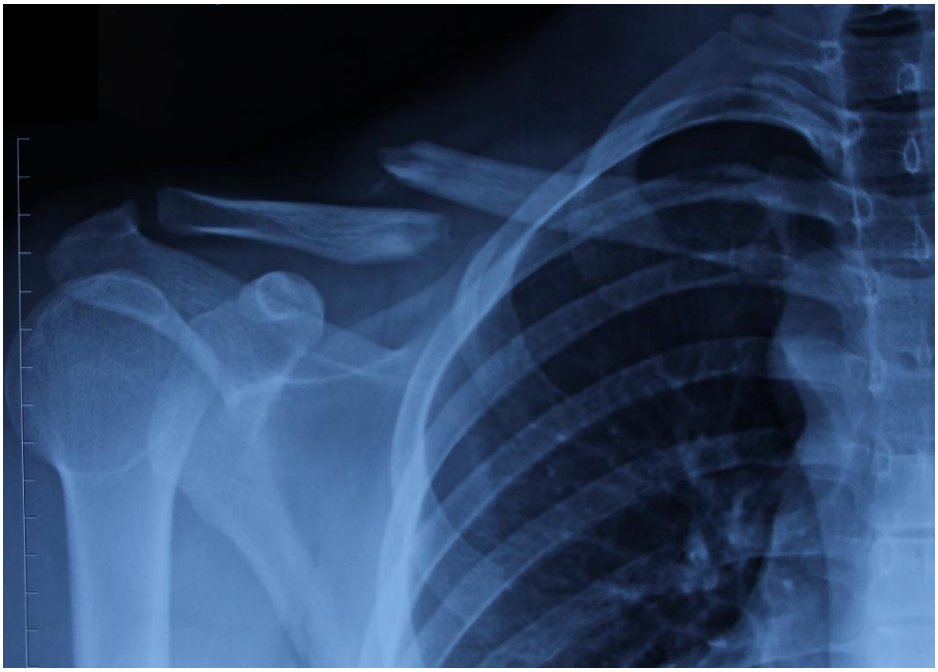

Figure 2 A displaced mid-shaft clavicle fracture.

The middle third of the clavicle shaft is noticeably narrower with a transitional area between the tubular medial end and the flattened lateral end of the clavicle, and this superficial region is not reinforced or protected by adjacent muscles and ligaments. Together, these factors make the clavicle vulnerable to mid-shaft fractures [20].

The relative positioning of the muscles attached to the clavicle is responsible for the clavicle's typical fracture pattern. In mid-shaft fractures the medial section is usually displaced superiorly as a result of the superior and posterior pulling forces of the sternocleidomastoid muscle, while the lateral segment is displaced inferiorly as a result of the inferior and anterior pull of the pectoralis major and deltoid muscles. The weight of the arm and shoulder also add to the inferior displacement of the lateral segment. In addition, the latissimus dorsi, trapezius and

pectoralis major muscles add medializing forces to the clavicle which result in clavicle shortening [18] [31] [20]. As a result of this pattern the clinical symptoms a patient would typically display are skin tenting over the medial segment, arm positioning in adduction across the chest, a shoulder droop, clavicle shortening, and mild internal rotation of the scapula. Very rarely are more serious complications reported in these types of fracture. Pneumothorax is only seen 3% of the time in high-velocity injuries. Neurovascular injuries may also occur, but are rare [20].

2.4.1 Current Methods of Diagnosis

Mid-shaft clavicle fractures are the easiest to visualize on plain film X-rays. The interpretation of the film should determine whether the fracture is comminuted, displaced, shortened or distracted. A computerized tomography (CT) scan of the clavicle are less common, but can help diagnose clavicle fractures and assess displacement if plain X-ray films are not clear [20].

2.4.2 Nonsurgical Treatment

Medial third clavicle fractures, being the rarest, are typically treated non-operatively because of the stability provided by the costoclavicular ligaments. This type of fracture is only treated surgically if there is severe displacement, open fracture, or if surrounding structures are at risk of injury [32] [33]. Lateral third clavicle fractures are typically stable with an intact periosteal sleeve, and are thus normally treated non-operatively [32]. Mid-shaft clavicle fractures are also most commonly treated non-operatively with an arm sling or brace for 2-6 weeks [20]. However, the high rates and wide range of non-union frequency (0.1% - 24%) observed in clavicle fractures reported by numerous recent studies may pose a problem to conservative treatment [34] [35] [36] [37]. Non-union is the failure to heal in fractured bones. It can occur for many

reasons, namely, displacement, comminution, shortening, bone instability, and poor nutrition and/or blood supply to fracture site [38] [3]. This complication is more prevalent in displaced fractures (15.1%) [35], and is proportional to the amount of displacement [37]. It can also lead to functional deficits such as poor arm abduction and shoulder muscle weakness [28, 31]. The evaluation of these poor outcomes, weighed against the risks of surgery have been investigated thoroughly, and it appears that together with the advancements in implant technology and surgical techniques, surgical reduction of clavicle fractures is becoming increasingly popular, especially for mid-shaft fractures [32, 39].

2.4.3 Surgical Treatment

While surgery is usually reserved for severe injuries with certain indications such as symptomatic non-union, stable fixation and bone grafts have been found to significantly improve non-union rates after failed conservative care [37] [34], especially when there is displacement involved [35]. In addition, clavicle fractures treated surgically have been found to improve functional outcome [33], and decrease pain and healing time allowing the patient to resume activity [40]. However, surgery has its drawbacks. Typical open reductions of the clavicle can be complicated by the nature of the procedure which involves long incisions and wide stripping [40]. Studies on surgical interventions of clavicle fractures have reported post-operative complications such as wound infections or dehiscence, neurovascular problems, deep infections and hardware malfunction. Infection rate can vary from 0% - 18%. Less common disadvantages are also seen, for instance, re-fracture, scarring and complex regional pain syndrome [3]. The development of minimally invasive techniques has proven effective in reducing these complications and are making surgical treatment a more favorable option [40].

There are many different approaches to clavicle fixation surgery and techniques. While mid-shaft clavicle fractures have been shown to heal properly non-operatively or with external fixation [41], internal fixation with plate osteosynthesis is the most widely used method, especially for displaced and/or comminuted mid-shaft clavicle fractures [42]. The most commonly used plates are locking plates (LP), dynamic compression plates (DCP), and Reconstruction plates [3]. Besides choosing the appropriate type of plate, many recent studies have evaluated the effects of different implant positions. At first plates were placed on the superior aspect of the clavicle, however, numerous studies have demonstrated the advantages of anteroinferior plate positioning [35] [43]. In addition to good implant stability and 94-100% union rate, the anteroinferior position reduces the risk of damaging infraclavicular structures with its screws, and decreases skin irritability over the clavicle [43] [44] [35]. The following are some of the most common hardware types:

- Dynamic compression plates (DCP): As the name implies, these plates apply compression to the bone as it heals. The drawback to these plates is that they need longer incision sites. Adequate implant stability, low hardware failure, and good bone healing rates have made these plates popular for treating clavicle fractures [45] [3] [44].
- Locking plates (LP): A problem with regular plates arises if the plate is not perfectly aligned to the contour of the bone. As the screw is tightened, one bone section may be pulled towards the implant, altering its position. However, the development of a locking screw mechanism into plates, which prevent this from occurring, has proven to be effective in the proper healing of clavicle fractures [45]. Furthermore, combining the positive effects of compression plates and the stability offered by locked plates, biomechanical studies have tested,

with good results, the outcome of locked compression plates [45] [3]. In vivo, both dynamic and locked compression plates offer similar positive results, but patients request the removal of the DCP more often [45].

- Intramedullary (IM) devices (Figure 3): The IM device, typically used to treat long bone fractures, is usually inserted through an anteromedial or postero-lateral entry point of the clavicle and lies inside the IM canal during fracture healing. However, the intricate shape and small diameter of the clavicle has complicated the development of effective IM devices. There is a wide variety of IM devices on the market that aim to attain the proper hardware strength while still being able to fit inside the IM canal [32]. The effectiveness of IM devices versus plate and screws has been heavily debated [46], but given the advancements in implant technology, recent meta-analysis results have suggested that IM devices are preferable for treating mid-shaft clavicle fractures [5] [6] [7]. Because the application of an IM device requires a smaller incision and is less invasive, it is associated with a reduced hospital stay and fewer complications [32] [46]. In addition, the fixation conserves the periosteum and surrounding soft tissue, and is aesthetically more pleasing as it does not protrude under the overlying skin. Most of the devices allow for its removal which is done with local anesthesia [32]. Furthermore, biomechanical studies have shown that both plates and IM devices are equally stable, but IM devices can be displaced more with larger loads [42] [47]. However, when this potential problem was investigated in vivo patient outcome evaluation scores, shoulder motion range, hardware failure, infection, non-union, and revision rates all showed no significant difference between plates and IM devices.

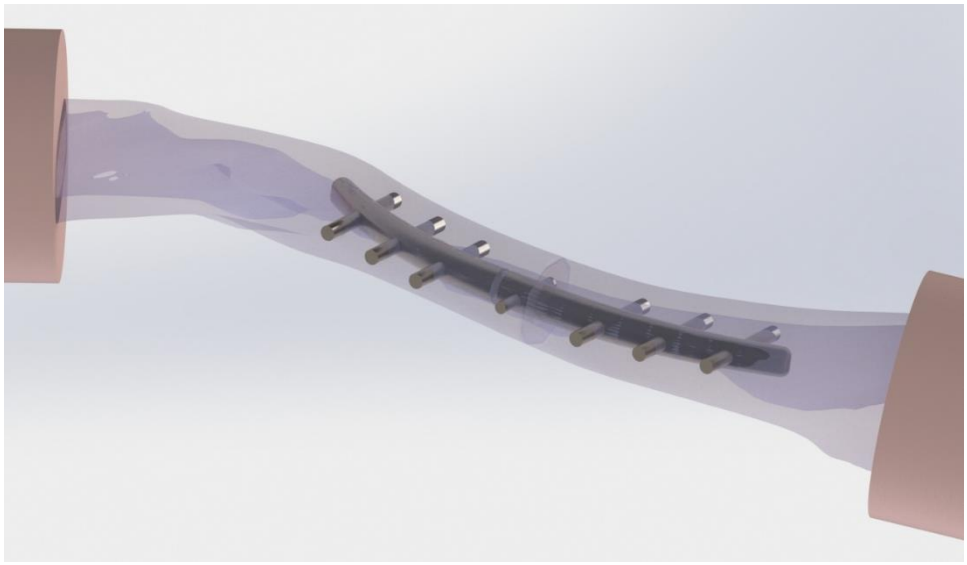

Figure 3 An IM device in the clavicle IM canal.

In addition, those treated with IM devices had less complications such as symptomatic hardware and re-fracture after hardware removal [5] [6] [7]. On the other hand, some biomechanical studies have reported problems with IM devices; they are less rotationally stable and may have pin migration [46].

2.4.4 Outcomes

Shoulder and arm functional problems that can result from clavicle shortening has been identified for a long time [21]. More recently, shoulder kinematic studies have found that clavicle discontinuity or shortening can change the moment arms of the muscles attached to the clavicle thus reducing their force capacity. The decreased force then hinders scapula mobility, including reduced external rotation, upward rotation and posterior tilting [28] [31]. However, studies using patient questionnaire scores argue on both sides whether or not there is a significant functional deficit after nonsurgical treatment of mid-shaft clavicle fractures [36] [48]. In conclusion, the increased awareness of functional deficit that can occur with severe mid-shaft fractures has

incented internal fixation of the clavicle [21]. Thus, current indications for internal fixation treatment have been established, such as more than 2 cm of shortening, over 100% displacement, high comminution, open fractures and floating shoulders [31].

2.5 Summary of Clavicle Morphometry Literature

For the measurements taken by the following studies in relation to clavicle anatomy, refer to Figures A.1 and A.2. The following studies are divided into 2 groups, starting with the 2-dimensional (2D) studies, followed by the 3-dimensional (3D) ones.

Andermahr et al. [8], obtained parameters using X-rays and calipers on 206 cadaveric clavicles, with grouping for gender and side. From the plain film they measured absolute clavicle length, depth of curvature and radius of curvature of the medial and lateral clavicle, diameter of the clavicle at the midpoint (50%), and diameters of the sternal and acromial ends. These locations along the clavicle were vaguely defined. After cutting through the specimens, cortex thickness and IM canal diameter were measured at different locations along the clavicle (approximately 15%, 25%, 33%, 50%, 66%, 75%, and 85% clavicle length). The diameter reported was the average between the height and width of the IM canal cross-section.

King et al. [11] had a very large in-vivo study with a sample size of 418 clavicles, matched for gender and grouping for age, gender and side. They used CT images of 1.25-2.5 mm slice thickness, but the type of measurement obtained was 2D from the axial, coronal and sagittal planes of the CT. The parameters measured were absolute clavicle length, angle of curvature in the axial and coronal planes, clavicle diameter height and width, and canal diameter height and width. However, the measurements were only taken at 3 vaguely defined points along the clavicle (approximately 15%, 50% and 83% clavicle length).

Another 2D study of the clavicle, by Mathieu et al. [9], studied clavicle morphometry with a sample size of 20 clavicles matched for gender and anatomical side. This study had an in-vivo and cadaveric sub-studies. The in-vivo portion used CT scans with no reported slice thickness or pixel size. The measurements were IM canal diameter height and width, taken in the sagittal plane at 7 vaguely defined points along the clavicle (approximately 15%, 25%, 33%, 50%, 66%, 75%, and 85%). The cadaveric portion of the study used calipers to measure clavicle absolute length, lateral and medial epiphysis and diaphysis diameter, lateral and medial clavicle depth of curvature, lateral and medial clavicle bending radius. There were no cadaveric IM canal measurements.

The first clavicle morphometry study by Bachoura et al. [46] was 2D. With a sample size of 22 cadaveric clavicles, they obtained CT scans of 0.6-0.2 mm slice thickness. The measurements were obtained from the sagittal planes of the CT and were not grouped by gender or side. The first parameter measured was absolute clavicle length from the “best fit” longitudinal axis along the clavicle. Next, they found the largest clavicle diameter and cortex thickness for each cross-section at the medial and lateral apex, and midpoint. These locations approximately corresponded to 40%, 80%, and 50% clavicle lengths respectively. Finally, the area of the IM canal in each cross-section was also calculated.

The study by Nourissat et al. [10] used a sample size of 20 in-vivo clavicle CT scans, but only the lateral end was examined. There was no grouping for gender or side, and slice thickness was 1.25 mm. The measurements were 2D, as they were obtained by re-slicing the CT scans: An axial view of the external third of the clavicle was used to estimate the center axis. Consequently, a new CT plane was calculated orthogonal to this axis in order to create slice clavicle cross-

sectional views at 5mm increments. The parameters measured were clavicle cross-sectional diameter, and the IM canal diameter. The latter was found by manually estimating the largest fit circle. However, results of this study cannot be compared to the present study as the cross-sectional slices were not taken at a consistent location along the clavicle.

Furthermore, Duprey et al. [17] examined 12 in-vivo clavicle CT scans with a slice thickness 1.25 mm and a pizel size of 0.283 – 0.791 mm. The measurement type of this anatomical study was 2D, taken from CT images with unspecified methods or procedure. The parameters measured were clavicle cross-section diameter at the midpoint (50%), medial and lateral end cross-section diameter (vaguely defined locations), absolute clavicle length, and radius of curvature and depth of curvature of the outer clavicle cortex.

However, Bernat et al. [12] analyzed the clavicle using a 3D method. With a sample size of 68 clavicles, matched for gender and side, this cadaveric study took CT images of 0.6 mm slice thickness and 0.5 mm pixel size. From the CT scans they computed a 3D coordinate system obtained from principal component analysis of the clavicle center line (CL). The CL was calculated using cylinder parameterization, and the parameters measured were true clavicle length, absolute length, clavicle cross-section width and height, and CL depth of curvature in the coronal and axial planes. No IM canal measurements were taken.

Bachoura et al. [13] later revisited their first clavicle study with a 3D analysis, using a similar sample size of 25 cadaveric clavicles without reporting gender or side. They obtained images using a laser scanner, and a CT for validation with slice thickness of 0.6-0.2 mm. The main longitudinal axis was obtained through a “best fit”. The absolute length of the clavicle was obtained along this axis. The points of maximum curvature were manually selected in the frontal

and axial planes, then the clavicle was divided into medial, middle and lateral thirds given these points. Next, the lengths of these segments were measured. Medial clavicle curvature was measured as an angle between the medial and middle segments, and lateral clavicle curvature was measured as an angle between the middle and lateral segments. Medial and lateral radius of curvature of the clavicle outside surface (not IM canal) was measured. Finally, the largest diameter at the mid-point of the clavicle (approximately 50%) was measured.

Daruwalla et al. [16] used a total sample of 21 clavicles; 9 of these were in-vivo CT scans, while the remaining 12 CTs were obtained from cadaveric specimens. All CTs used 0.625 mm slice thickness. The coordinate system was created by selecting landmarks to create a best fit plane (approximately axial) on the lateral flat surface of the clavicle, and creating a plane (approximately sagittal) perpendicular to a line connecting the medial and lateral ends of the clavicle. The clavicle was then sliced into 50 sections using the sagittal planes. Then the centers of each cross section were used to create a best-fit longitudinal axis. The measurement type is 3D and the parameters reported were absolute clavicle length, and cross-sectional clavicle diameter (not IM canal) obtained by averaging the cross-section height and width at various clavicle locations (10%, 50% and 90%). The study also reported statistical shape modeling results and cluster division using principal component analysis.

Daruwalla et al. [15] published a second paper on 3D clavicle morphometry in a different journal. Instead of the statistical shape models, they reported more clavicle parameters. The methods for obtaining these additional results were very similar. They measured clavicle (not IM canal) cross-sectional diameter height and width at various clavicle locations (10%, 20%, 30%,

40%, 50%, 60%, 70%, 80% and 90%). The study also reported depth of curvature of the outer cortex and angle of curvature.

Abdel Fatah et al. [14] created an anatomical atlas and statistical model for the study of 3D shape of the clavicle. They used CT scans of 1010 cadaveric clavicles, 570 male and 440 female, matched for side. However, the purpose of this study was to create and validate the anatomical atlas and as such authors did not report on individual clavicle parameters. Additionally, the validation of the segmentation process from CTs was done.

Finally, Lu and Untaroiu [22] analyzed the variation in clavicle shape using a statistical approach. Their models were obtained from CT scans of 20 left-sided cadaveric clavicles; gender was not specified, CT thickness was 0.625 and pixel size 0.2 mm. The parameters measured were distribution of shapes, model compactness, model generalization and specificity, and clavicle absolute length.

CHAPTER 3: CLAVICLE MORPHOMETRY STUDY

3.1 Study Population

All patient included in this basic science study had shoulder computed tomography (CT) scans done prior as part of their diagnostic examination not related to this study. Therefore this is a retrospective study. The inclusion criteria includes the following: entire clavicle (from lateral to medial end) in the field of view, slice thickness lower or equal to 1 mm, no congenital malformation of the clavicle, no acute or healed fracture of the clavicle or previous clavicle-related surgery, and no metal present in the field of view. Orthopedic fellows verified the presence of bony abnormalities. A total of 104 clavicles met the criteria, 51 male (age range 33-82 years old, average 63.8±11.0 years); and 53 female (age range 40-86 years old, average 66.8±10.9 years). Additionally, study population consists of 54 right clavicles (28 male, 26 female) and 50 left clavicles (23 male, 27 female).

All examinations were performed on a GE Lightspeed QZ/i Helical Scanner (GE Healthcare, Waukesha, WI, USA) in the supine position. The CT images included in this study were acquired from the affiliated hospital database and standard protocol to de-identify the subjects was followed. The scans were taken in an axial view with scanning parameters ranging from 0.625-1.0 mm slice thickness and 0.383-0.619 mm pixel size. The images were stored in Digital Imaging and Communications in Medicine (DICOM; National Electrical Manufacturers Association, Rosslyn, VA, USA) format and then transferred to computers for analysis.

3.2 Methodology

3.2.1 Segmentation, Standardization and Normalization

Segmentation: Using a standardized protocol, three distinct 3D models of the clavicle were created in MIMICS (Materialise, Leuven, Belgium) by the same operator. Firstly, for each clavicle the Hounsfield Unit (HU) value corresponding to the cortex of the clavicle was established as a threshold level separating the clavicle from surrounding soft tissue. Consequently the entire clavicle is filled in and a solid model is generated. This can be seen in Figure 4 a and b. Secondly, HU values below cortex level (corresponding to trabecular bone, IM canal, soft tissue, etc.) were used to constitute the non-cortical model (trabecular bone and IM canal) within the clavicle, as seen in Figure 4 c and d. Finally, the third model was created from a Boolean operation between the first two. The IM canal was subtracted from the solid clavicle to generate the cortical bone model in Figure 4 d. It was done in this fashion to make sure all voxels in the clavicle model were accounted for properly. No voxel was included twice, once in the cortical model and again in the IM canal model, and no voxel was missing from either model. The solid and cortical models were exported in text file format as volumetric model (Figure 4 b, f) and as point-cloud surface models (Figure 5).

Refer to Table C.1 for a list of terminology used in this section. A custom-written automatic algorithm (MATLAB, MathWorks, Natick, MA) was utilized for the subsequent data analysis:

- Standardization: A subject-specific coordinate system was established for each clavicle. This was done using principle component analysis (PCA) on the volumetric model of the solid clavicle. PCA works by calculating the covariate matrix of the data, then uses that to find its

eigenvectors and eigenvalues. The first eigenvector, also called the principal component, points in the direction of greatest variance in the data. The magnitude of this vector is its eigenvalue.

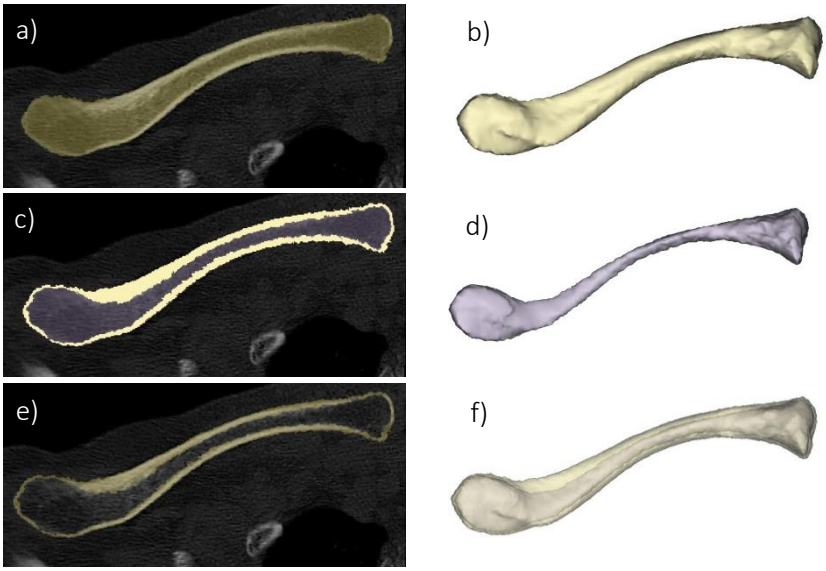

Figure 4 Segmentation process of a clavicle from the CT scan. a) Highlighted solid clavicle. b) Volumetric model of the solid clavicle. c) Highlighted IM canal. d) Volumetric model of the IM canal. e) Cortical layer obtained by subtracting IM canal from solid clavicle. f) Volumetric model of the clavicle cortex.

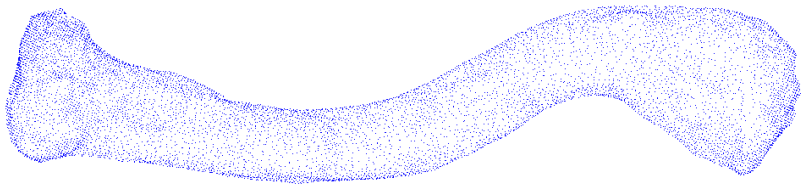

Figure 5 A point cloud surface model of the solid clavicle.

The second eigenvector points in the direction of greatest variance of data orthogonal to the first. Additional eigenvectors are calculated until their number equals the number of variables in the data. Figure 6 shows a 2D example of how PCA is applied. In the case of the current study, the data pertaining to the location of each voxel of the clavicle model in Euclidian space was

subjected to PCA, and yielded three principal directions. The first was along the longitudinal axis 'z' (1st principal direction), in the approximately anterior-posterior direction 'y' (2st principal direction), and in the approximately superior-inferior direction 'x' (3st principal direction), as seen in Figure 7.

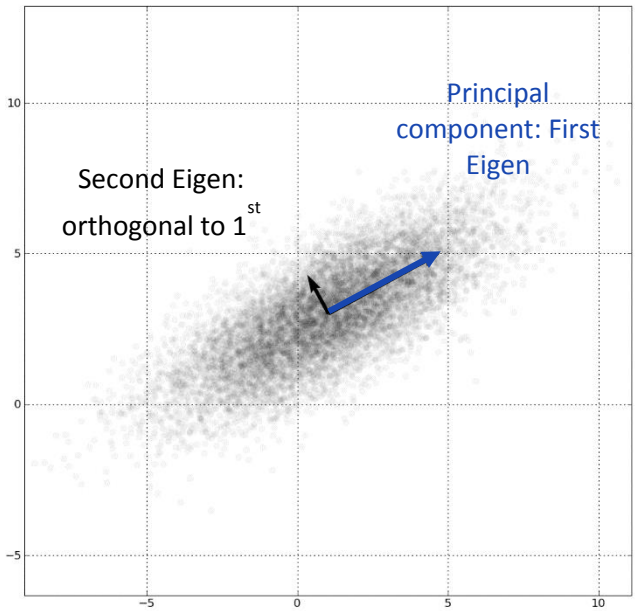

Figure 6 2D example of the application of PCA. The principal component points in the direction of maximum variance. Adapted from [49]

The unique shape of the clavicle (s-shaped in the transverse plane view [' $y_G z_G$ '], relatively straight in coronal plane view [' $x_G z_G$ ']) is advantageous when employing PCA, as all 3 calculated components will point in the same direction for all clavicles, allowing them to be compared effectively to each other. The geometric center 'C' of the clavicle volumetric model was calculated for each subject using (1) where, 'C = [C_x, C_y, C_z]', and N = number of voxels in each model.

$$C_x = \frac{1}{N}\sum_i^N x_i \; ; \; C_y = \frac{1}{N}\sum_i^N y_i \; ; C_z = \frac{1}{N}\sum_i^N z_i \qquad (1)$$

Subsequently, using orthogonal transformation every clavicle model (solid, IM canal, and cortical in both volumetric and surface versions) was converted from global coordinate system (['x_G,y_G,z_G'] - CT established) into new local coordinate system (['x_L,y_L,z_L'] – PCA established) with geometric center of the clavicle to be set at local coordinate system origin 'C=[0,0,0]'. This was done by first translating (2) the models so the geometric center is located at origin, then rotating (3) them to the new local axes, where p1 is the principal component, p2 the second, and p3 the third.

$$\begin{bmatrix} x_{Gc} \\ y_{Gc} \\ z_{Gc} \end{bmatrix} = \begin{bmatrix} x_G \\ y_G \\ z_G \end{bmatrix} - \begin{bmatrix} C_x \\ C_y \\ C_z \end{bmatrix} \tag{2}$$

$$\begin{bmatrix} x_L \\ y_L \\ z_L \end{bmatrix} = \begin{bmatrix} p3 \cdot \boldsymbol{i}' & p3 \cdot \boldsymbol{j}' & p3 \cdot \boldsymbol{k}' \\ p2 \cdot \boldsymbol{i}' & p2 \cdot \boldsymbol{j}' & p2 \cdot \boldsymbol{k}' \\ p1 \cdot \boldsymbol{i}' & p1 \cdot \boldsymbol{j}' & p1 \cdot \boldsymbol{k}' \end{bmatrix} \begin{bmatrix} x_{Gc} \\ y_{Gc} \\ z_{Gc} \end{bmatrix} \tag{3}$$

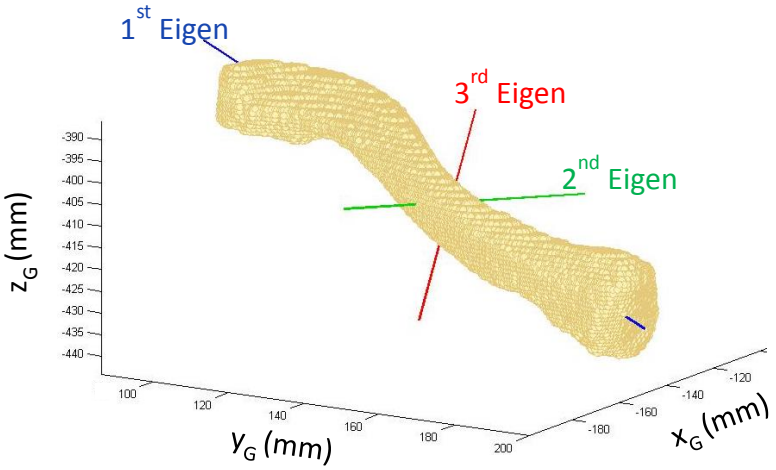

Figure 7 First, second and third components calculated on the solid clavicle model in global (original) coordinate system.

Thus, the three components constituting orthogonal subject-specific coordinate system were aligned with axes of local coordinate system as follows: '$z=z_L$; $y=y_L$; $x=x_L$'. This is shown in Figure 8 a, and the original position is shown in Figure 7.

The final step in the standardization process involved inverting the longitudinal axis 'z_L' with respect to the '[x_L,y_L]' plane in only left-sided clavicles, as seen in Figure 8 b, yielding the right-sided version of the clavicle. This step was necessary as it allowed all clavicles in the sample population to be compared to each other regardless of side.

- Normalization: In order to examine the morphometric parameters of all clavicles of varying sizes, they had to be normalized with respect to length. This was accomplished by creating a tightest-fit orthogonal bounding box around every clavicle model, as seen in Figure 9. The vertical length of the box (L_z) represents 100% of the clavicle absolute length. The box was then divided into a hundred slices perpendicular to the box's vertical length (L_z).

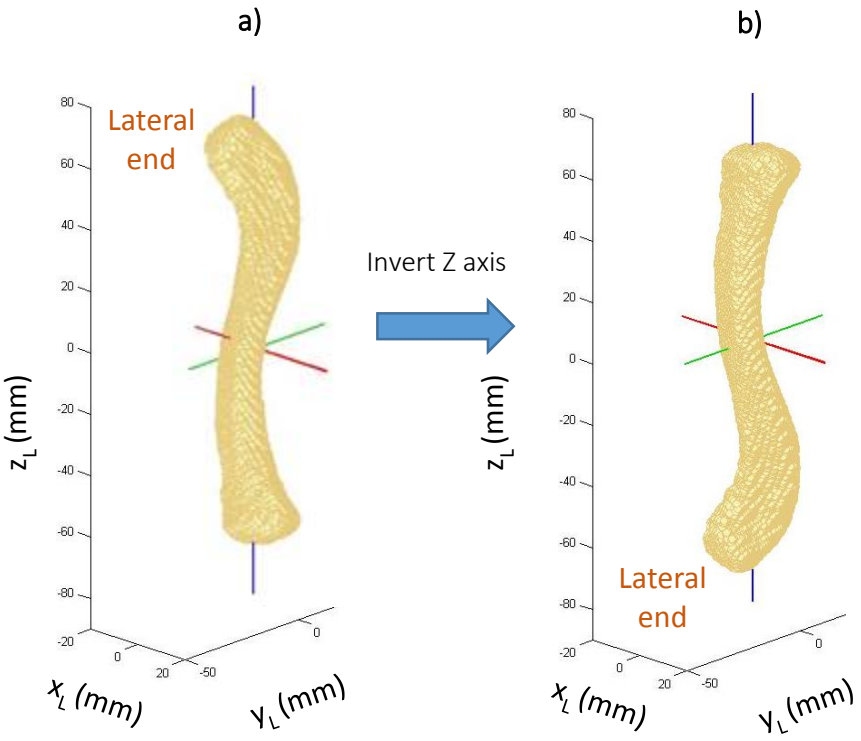

Figure 8 Clavicle models in local coordinate system after orthogonal transformation. a) Original-sided (left) version of clavicle with 'C=[0,0,0]' b) Mirror image (right) of clavicle with 'C=[0,0,0]'.

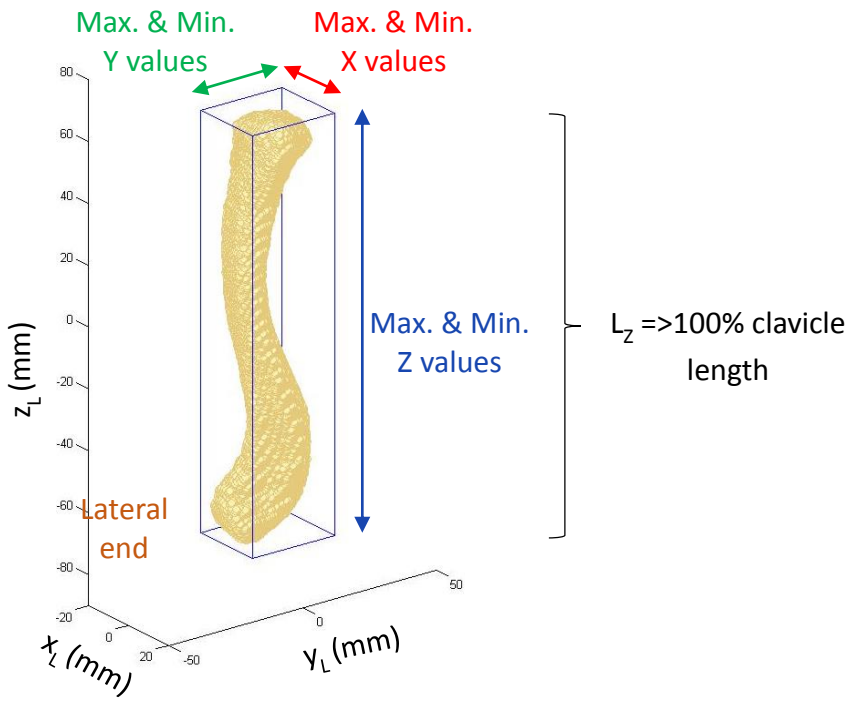

Figure 9 Normalization with tightest-fit orthogonal-bounding box. Bounding values for each axis were selected from the maximum and minim values of the volumetric solid clavicle model.

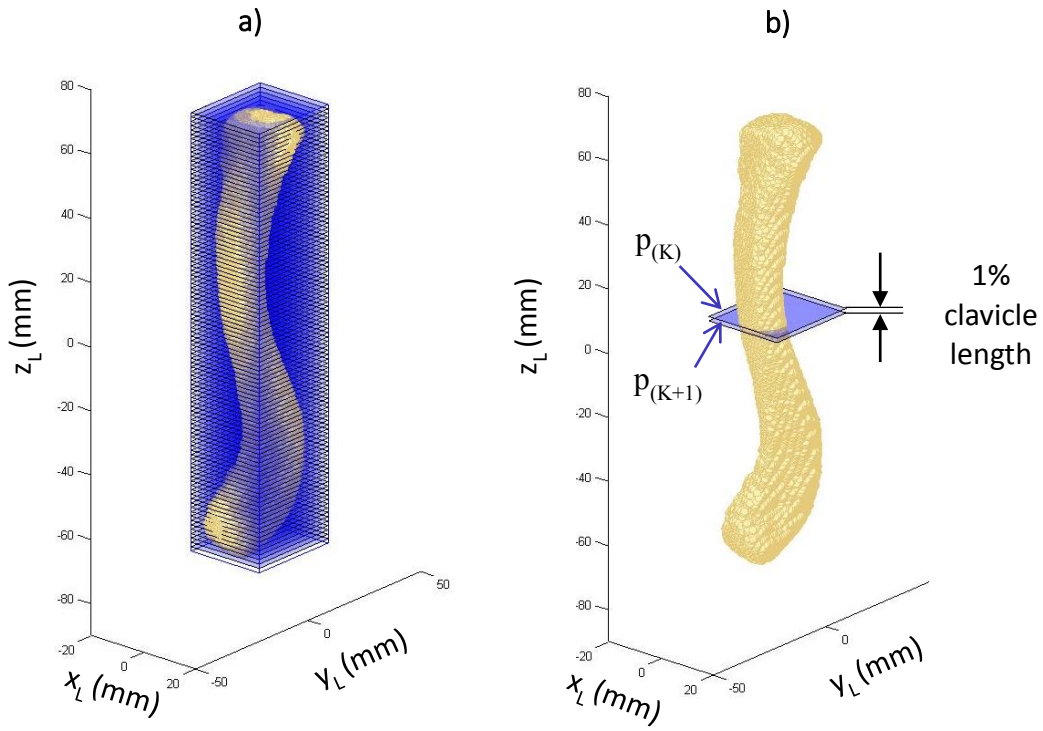

Figure 10 Slicing tightest-fit box into 100 sections parallel to the '[x_L,y_L]' plane (a). Each resulting section, between planes $p_{(K)}$ and $p_{(K+1)}$, represents 1% clavicle thickness (b).

Each slice was created by a '[x_L,y_L]' plane at increments equal to 1/100 of its absolute length (L_z/100) starting at the top of the box on sternal (medial) end of the clavicle. As a result, each slice thickness represents 1% clavicle length. This process can be seen in Figure 10.

3.2.2 Circumscribed and Inscribed Circle Calculation

The morphometric parameters were evaluated on the normalized clavicle cortex and solid models. Clavicle and IM canal diameters were measured as a function of normalized clavicle length at every 1/100 of its absolute length. Points lying between a pair of consecutive planes $p_{(K)}$ and $p_{(K+1)}$ for both clavicle cortex and solid models were projected on $p_{(K+1)}$ in Figure 11. Next, the 2D solid model points projection was fitted with a tightest fit circumscribed circle that approximated clavicle cross-section dimensions. The algorithm responsible for creating this circle first calculated the smallest convex set containing points in the Euclidean plane $p_{(K+1)}$ (convex hull envelope). Consequently, a minimal radius enclosing circle was calculated for this set of points,

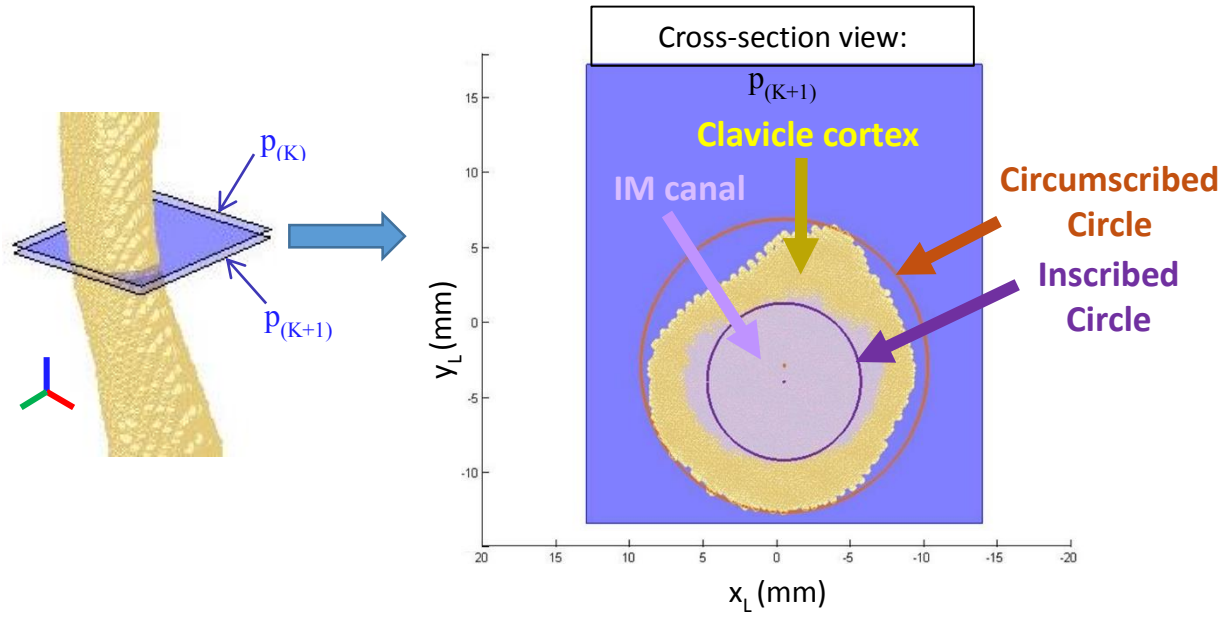

Figure 11 Projection of clavicle slice K onto $p_{(K+1)}$ and fitted with circumscribed and inscribed circles.

Under the rule that it must pass through at least 3 points in the set and exclude none. Radius $\mathbf{r_i}$ and center position $\mathbf{C_c} = [x_{Cc}, y_{Cc}, z_{Cc}\ (\text{func}\ (L_z)_{Cc})]$ was found for every point projection.

On the other hand, the inscribed circle was calculated for every cortex slice points projection using an algorithm to find the maximum radius circle fitted inside the convex set of points. The algorithm responsible for this calculates the Convex Hull around the point cloud surface of the IM canal, then creates a Voronoi diagram with that point set. A Voronoi diagram divides the area into regions containing one point (called a seed) based on the distance between other adjacent points. Thus, a Voronoi edge, a line of contact between two adjacent Voronoi regions, is equidistant between two seeds. In a similar fashion, a Voronoi edge is the point of intersection of 3 regions, and is equidistant between 3 seeds. This is illustrated in Figure 12.

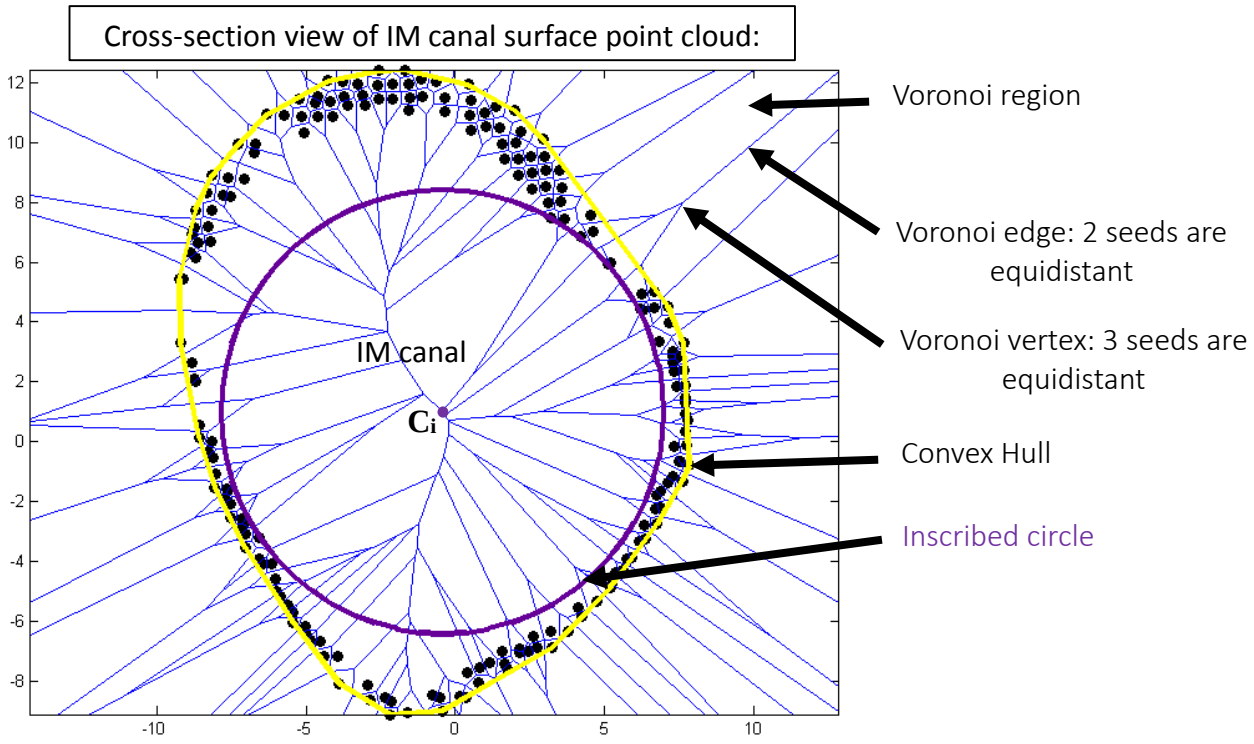

Figure 12 Voronoi diagram and Convex Hull computed for a single slice projection of the IM canal surface point cloud, and the resultant maximized inscribed circle.

Given all the vertices located inside the Convex Hull, the algorithm finds the one that yields a circle with the largest radius $\mathbf{r_i}$ without crossing the Convex Hull or including any other points inside of it. This circle's center position is given by $\mathbf{C_i} = [x_{ci}, y_{ci}, z_{ci}(\text{func } (L_z)_{ci})]$. Finally, this calculation was performed for every slice point projection between 10-90% of clavicle absolute length L_z. Initial and final 10% of the clavicle length were not considered as they do not represent IM canal, but trabecular bone. The percentages were established empirically based on the difference in densities of the trabecular bone and the IM canal at the lateral and medial ends [11].

3.2.3 Other Clavicle Parameters

The radius of curvature of the IM canal was measured at the centerline ($\mathbf{CL_i}$) created by centers of inscribed circles ($\mathbf{C_i}$) between 10-90% of clavicular length ($\mathbf{L_z}$). The curvature in the coronal plane ('x_Lz_L') was neglected. $\mathbf{CL_i}$ was projected onto transverse plane ('y_Lz_L') and the inflection point was determined from the center displacement results; this was the point of intersection between $\mathbf{CL_i}$ and 'z_L'. Using this point, was divided into the convex medial section and the concave lateral section. Using the least squares method, the radius of curvature was estimated for each section. This is shown in Figure 13.

The absolute length of the clavicle was measured as total vertical length of the bounding box **Lz**, as shown in Figure 14. The true length of the clavicle was measured for each subject along the centerline $\mathbf{CL_c}$ created by circumscribed circle centers $\mathbf{C_c}$. This was accomplished by finding the distance between adjacent $\mathbf{C_c}$, and adding all of them together.

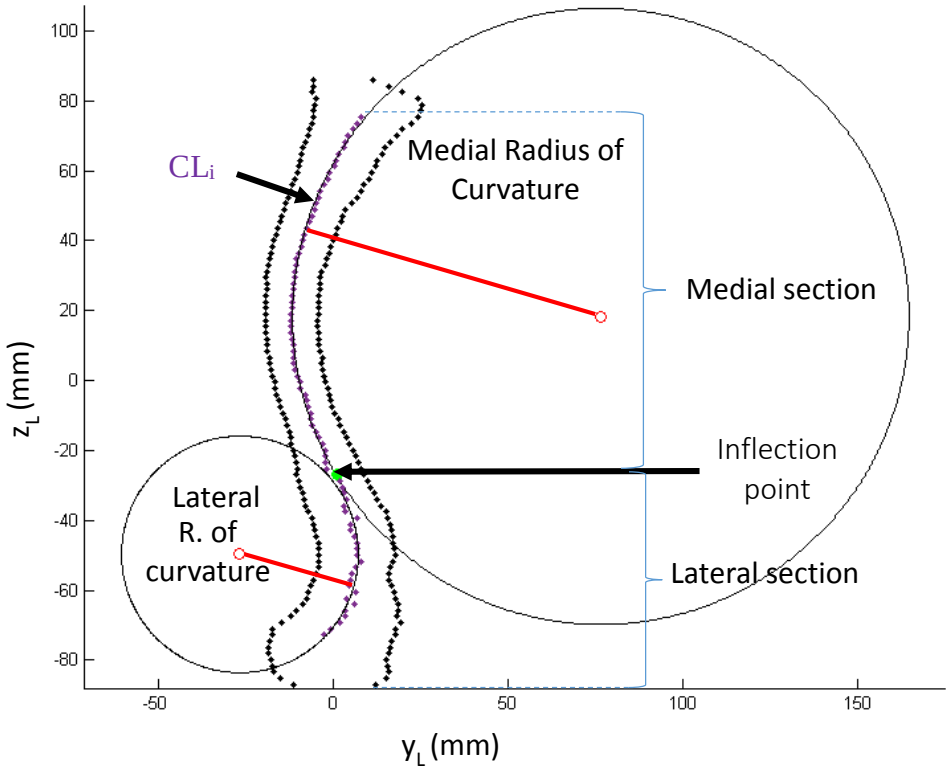

Figure 13 Radius of curvature of the IM canal for both medial and lateral sections. **CL_i** is given by the collective **C_i** for each clavicle.

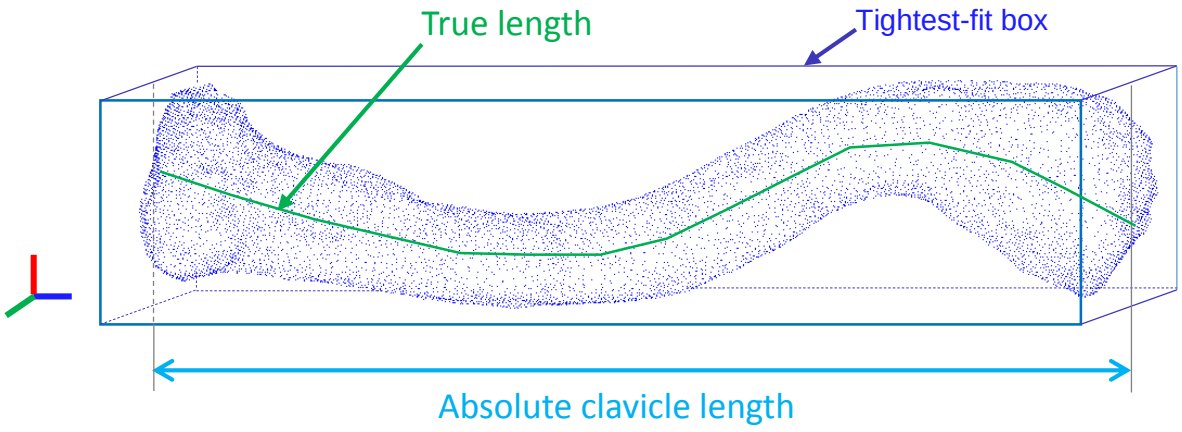

Figure 14 Absolute and true clavicle lengths. The true length is the cumulative distance between centers C_i, while absolute length is the longitudinal length of the tightest-fit box.

3.2.4 Statistical Analysis

Averages, standard deviations, ranges, minimum values and maximum values were calculated for every studied parameter. Furthermore, an unpaired t-test (significance level alpha = 0.05) was utilized to evaluate the effect of gender and side within each studied parameter. In addition, the Pearson correlation coefficient was calculated to evaluate the correlation between true and absolute clavicle length.

3.3 Results

All parameters were compared with respect to gender and anatomical side. In addition, all parameters (except for circle center displacement results) comparable to those of previous studies have been tabulated in detail in Appendix A.

3.3.1 Clavicle and Intramedullary Canal Radius

The radius of all 100 circumscribed circles fitted along the clavicle were reported as a function of percent clavicle length, starting (1%) at the medial end of the clavicle. Because the circumscribed circles enclose the bone in its entirety, their diameters represent the largest clavicle diameter at any given cross-section. Figure 11 illustrates the relationship between circles and bone cross-section. Results for all subjects are shown in Figure 15. Overall, the average minimal largest radius of the clavicle was 6.86 mm at 49% of its length. Moreover, the average minimal largest radius of the clavicle was 7.76±0.66 mm at 46% length for males and 5.99±0.64 mm at 48-49% length for females ($p<.0001$) (Figure 16). When grouping for anatomical side, the minimal largest radius was 7.05±1.08 mm at 48% length for right-sided clavicles, and 6.72±1.04 mm at 40-41% length for left-sided clavicles (Figure 17) ($p=.0737$). In addition, circumscribed radii of right-sided clavicles were larger for both genders ($p=.081$) (Figure 18).

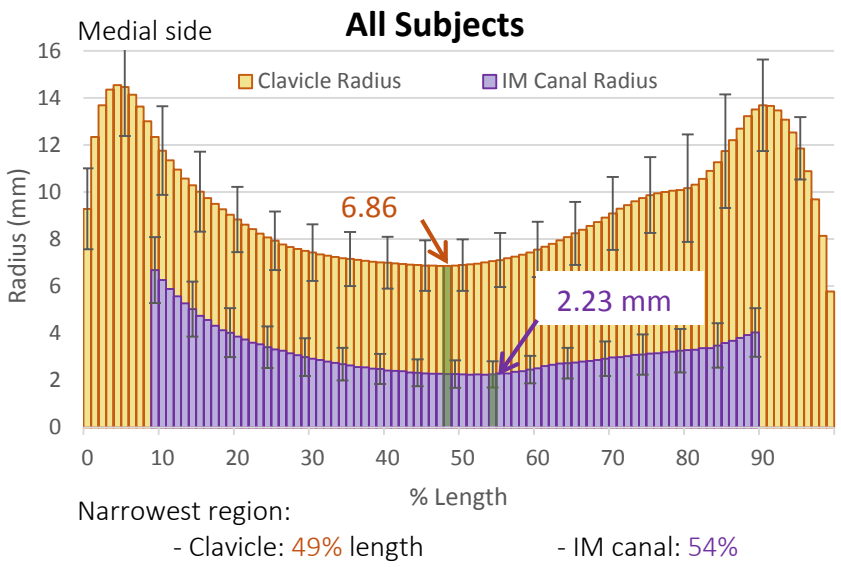

Figure 15 Average radius of circumscribed and inscribed circles for all subjects as a function of clavicle length with standard deviation. The narrowest regions are highlighted.

Similarly, inscribed radii fitted along the clavicle were reported as a function of percent clavicle length, starting (1%) at the medial end of the clavicle. However, the diameter of these circles represent the smallest IM canal diameter at any given cross-section (Figure 11). Results for all subjects are shown in Figure 15. Overall, the narrowest region of the IM canal had a radius of 2.23±0.57 mm at 54% clavicle length. Furthermore, the narrowest region of the IM canal had a radius of 2.55±0.47 mm at 54% clavicle length for males, and a radius of 1.92±0.46 mm at 52% clavicle length for females (Figure 16) ($p<.0001$). When grouping for anatomical side, the smallest radius was 2.36±0.51 mm at 54-55% length for right-sided clavicles, and 2.10±0.57 mm at 54% length for left-sided clavicles (Figure 17) ($p=.052$). In addition, inscribed radii of right-sided clavicles were larger regardless of gender (Figure 18). This finding was also statistically insignificant ($p=.048$).

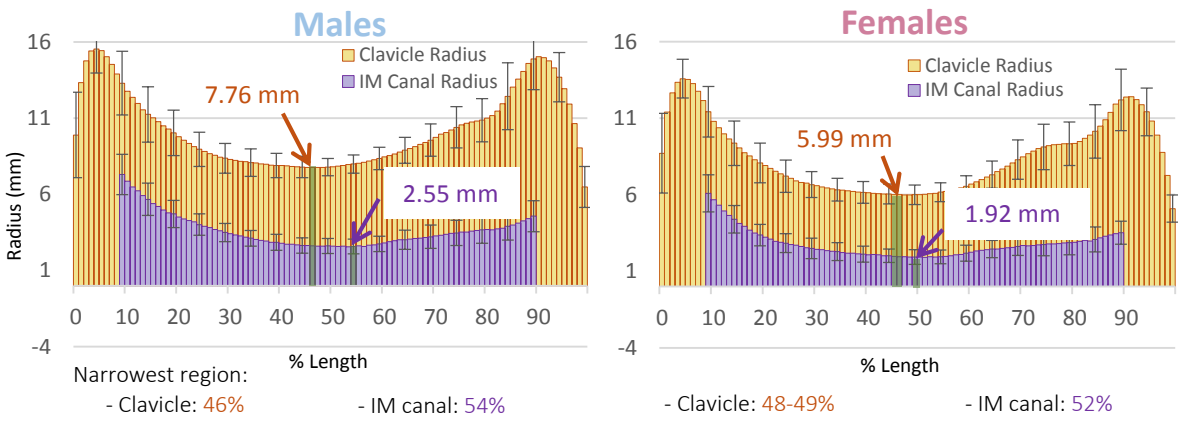

Figure 16 Average radius of circumscribed and inscribed circles grouped by gender. The narrowest regions are highlighted

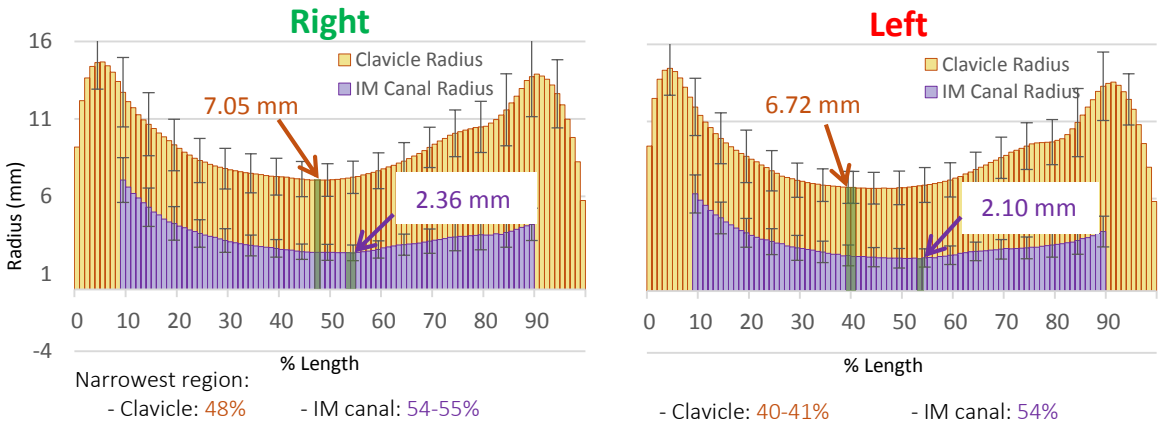

Figure 17 Average radius of circumscribed and inscribed circles grouped by side. The narrowest regions are highlighted.

3.3.2 Clavicle and Intramedullary Canal Center Displacement

The following results are divided into clavicle and IM canal center displacement:

- Clavicle: the calculated centers ($\mathbf{C_c}$) of the circumscribed circles, together forming the center line of the clavicle ($\mathbf{CL_c}$), where measured as displacements from 'z_L' in the 'y_L' direction. Thus, displacement results are projected onto the [y_L,z_L] plane with 'y_L' displacement being a function of clavicle length along 'z_L'. $\mathbf{CL_c}$ was divided into two sections, the medial and

lateral curvatures. In the medial curvature, as seen in Figure 19, its centers are displaced in the negative 'y_L' direction; this corresponds to an approximately anterior anatomical displacement,

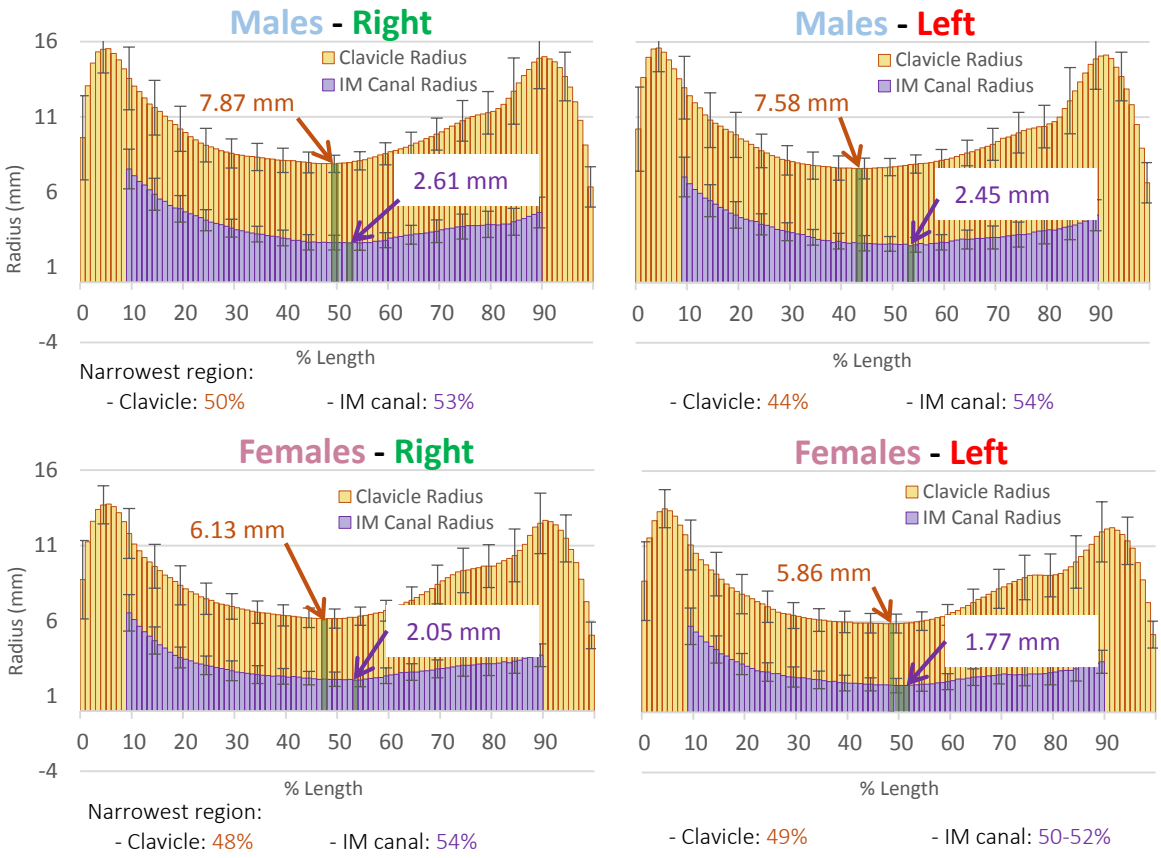

Figure 18 Average radius of circumscribed and inscribed circles grouped by gender and anatomical side. The narrowest regions are highlighted.

while positive values, seen in the lateral curvature, correspond to an approximately posterior direction. Understanding this, the sign is ignored and only absolute values are reported. Firstly, in the medial curvature the overall maximum displacement of $\mathbf{C}_c$ was 7.32±1.47 mm at 36-39% clavicle length (Figure 19). Maximum displacement of $\mathbf{C}_c$ was 7.73±1.26 mm at 37% length for females, and 8.21±1.54 mm at 39% length for males (Figure 20) (p=.0013). When grouped by anatomical side, maximum displacement of $\mathbf{C}_c$ was 7.79±1.44 mm at 39% length for right-sided

clavicles, and 7.74±1.46 mm at 37% for the left-sided (Figure 21) (p=.8879). Additional results after grouping by gender and side can be seen in Table 1.

Secondly, for the lateral segment the overall maximum displacement of $\mathbf{C}_c$ was 4.65±1.53 mm at 76-77% clavicle length (Figure 19). Maximum displacement of $\mathbf{C}_c$ was 4.07±1.33 mm at 77% length for females, and 5.28±1.44 mm at 76% length for males (Figure 20) (p<.0001). When grouped by anatomical side, maximum displacement of $\mathbf{C}_c$ was 4.52±1.40 mm at 76% length for right-sided clavicles, and 4.81±1.60 mm at 77% for the left-sided (Figure 21) (p=.2761). Further results after grouping by gender and side can be seen in Table 1.

- IM canal: Similarly, the calculated centers ($\mathbf{C}_i$) of the inscribed circles, together forming the center line of the clavicle ($\mathbf{CL}_i$), where measured as displacements from 'z_L' in the 'y_L' direction. Also, $\mathbf{CL}_i$ was divided into two sections, the medial and lateral curvatures. For the medial segment of the IM canal, the overall maximum displacement of $\mathbf{C}_i$ was 7.78±2.25 mm at 37% clavicle length (Figure 19). Furthermore, maximum displacement of $\mathbf{C}_i$ was 7.18±2.56 mm at 36% length for females, and 8.42±1.60 mm at 37% length for males (Figure 20) (p=.0015). When grouped by anatomical side, maximum displacement of $\mathbf{C}_i$ was 7.99±1.57 mm at 38% length for right-sided clavicles, and 7.61±2.85 mm at 37% for the left-sided (Figure 21) (p=.892). Results after grouping by gender and side can be seen in Table 1.

Within the lateral segment the overall maximum displacement of $\mathbf{C}_i$ was 6.56±2.12 mm at 78-79% clavicle length (Figure 19). Maximum displacement of $\mathbf{C}_i$ was 5.90±2.34 mm at 78% length for females, and 7.27±1.84 mm at 79% length for males (Figure 20) (p<.0001). When grouped by anatomical side, maximum displacement of $\mathbf{C}_i$ was 6.69±1.86 mm at 79% length for right-sided

clavicles, and 6.55±2.52 mm at 78% for the left-sided (Figure 21) (p=.8885). Results after grouping by gender and side can be seen in Table 1.

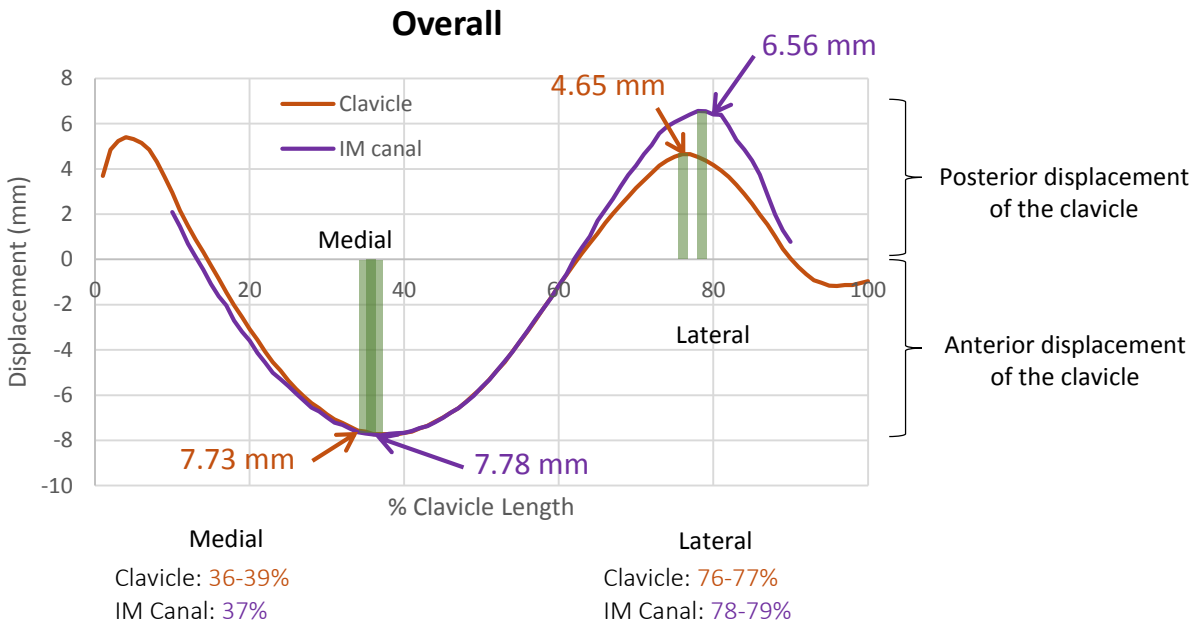

Figure 19 Overall average displacement of circumscribed centers ($\mathbf{C_c}$) and inscribed centers ($\mathbf{C_i}$) in 'y_L' direction. The maximum values for the medial and lateral curvatures are highlighted.

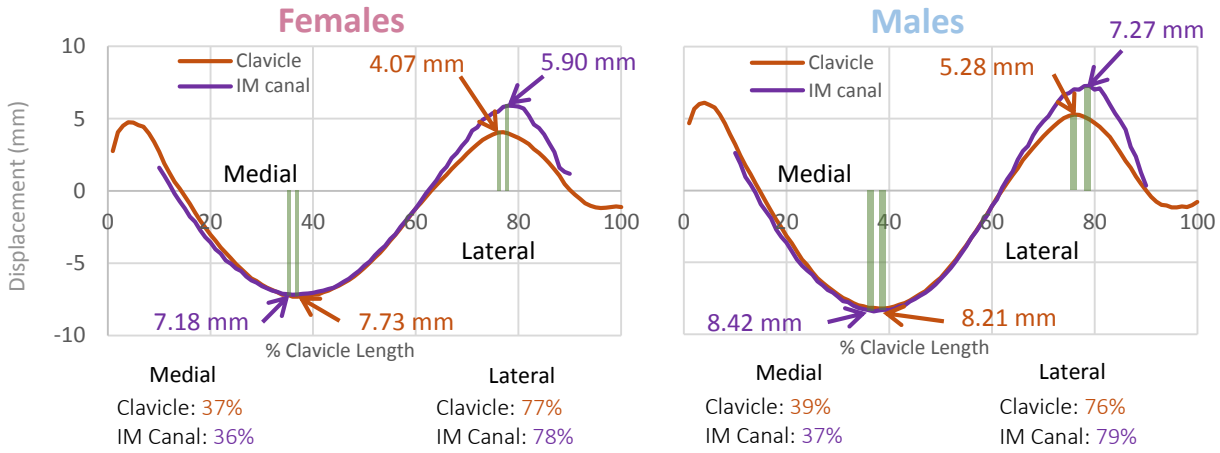

Figure 20 Average displacement of circumscribed centers ($\mathbf{C_c}$) and inscribed centers ($\mathbf{C_i}$) in 'y_L' direction when grouped by gender. The maximum values for the medial and lateral curvatures are highlighted.

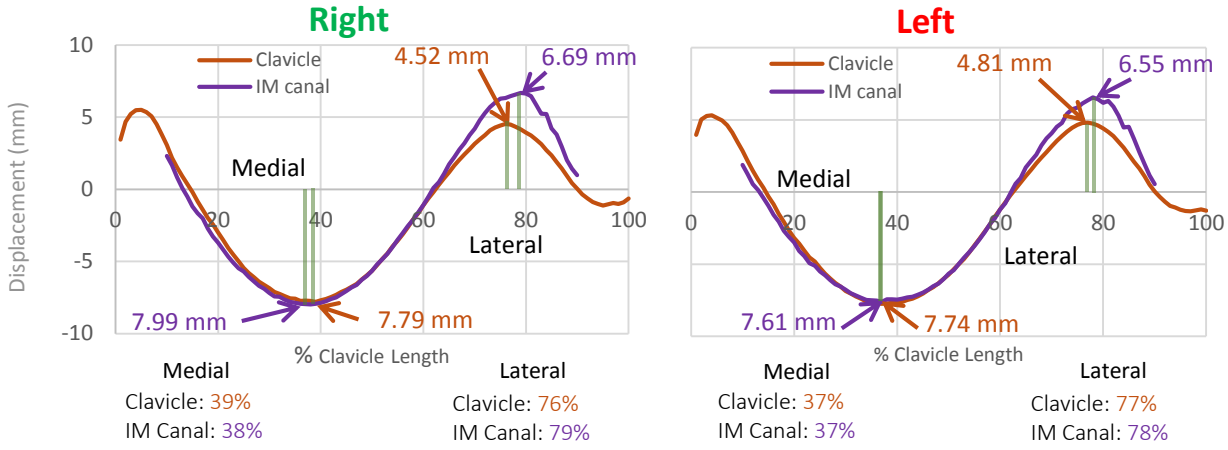

Figure 21 Average displacement of circumscribed centers ($\mathbf{C_c}$) and inscribed centers ($\mathbf{C_i}$) in 'y_L' direction when grouped by anatomical side. The maximum values for the medial and lateral curvatures are highlighted.

Table 1 Displacement and standard deviation of circumscribed centers ($\mathbf{C_c}$) and inscribed centers ($\mathbf{C_i}$) in 'y_L' direction when grouped by anatomical side and gender.

Segment		Females - Right		Females - Left	
		DISP (mm) ±SD	Slice	DISP (mm) ±SD	Slice
Medial	Clavicle	**7.51 ± 1.03**	**39%**	**7.21 ± 1.50**	**37%**
	IM Canal	**7.71 ± 1.05**	**36%**	**6.72 ± 3.40**	**37%**
Lateral	Clavicle	**4.11 ± 1.33**	**77%**	**4.03 ± 1.36**	**77%**
	IM Canal	**6.26 ± 1.34**	**80%**	**5.77 ± 2.80**	**78%**

Segment		Males - Right		Males - Left	
		DISP (mm) ±SD	Slice	DISP (mm) ±SD	Slice
Medial	Clavicle	**8.05 ± 1.71**	**39%**	**8.45 ± 1.30**	**38%**
	IM Canal	**8.28 ± 1.86**	**38%**	**8.52 ± 1.43**	**41%**
Lateral	Clavicle	**4.90 ± 1.34**	**76%**	**5.76 ± 1.37**	**77%**
	IM Canal	**7.21 ± 1.99**	**79%**	**7.50 ± 1.76**	**78%**

Finally, the center lines $\mathbf{CL_c}$ and $\mathbf{CL_i}$ were also examined in the $[x_L,z_L]$ plane, so displacements of $\mathbf{C_c}$ and $\mathbf{C_i}$ were measured from 'z_L' in the 'x_L' direction. Maximum clavicle center displacement was 2.57±1.67 mm at 63% clavicle length, and maximum IM canal center

displacement was 2.82±1.78 mm at 66% clavicle length (Figure 22). Because these maximum values were small, displacements in the 'x_L' direction were not investigated further.

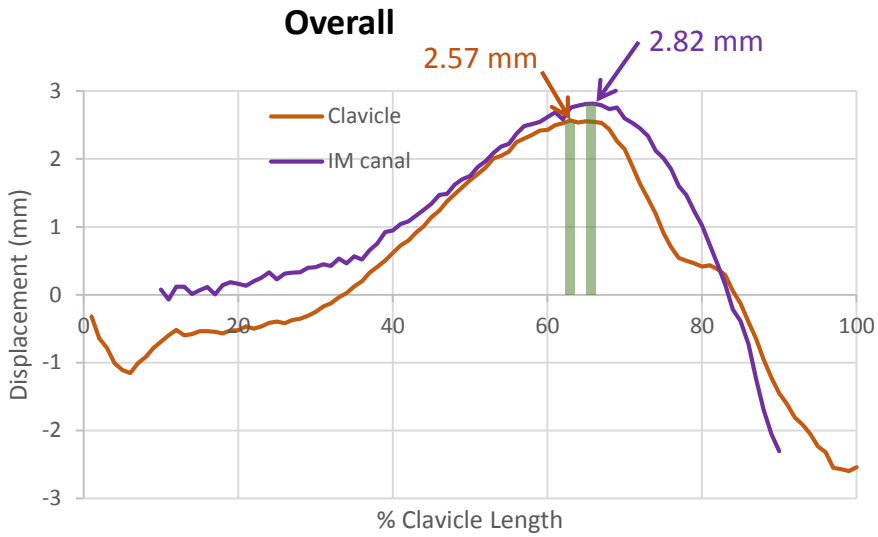

Figure 22 Average displacement of circumscribed centers (**C_c**) and inscribed centers (**C_i**) in 'x_L' direction for all subjects. The maximum values are highlighted.

3.3.3 Intramedullary Canal Radius of Curvature

The mean radius of curvature of the IM canal was measured at the transverse ('$[z_L,y_L]$') plane (defined by primary directions derived from principal component analysis), and reported for each segment:

- Medial segment: Mean radius of curvature for wall subjects was 91.19±14.38 mm (range: 56.88-139.85 mm; Table 2). Male IM canals had a significantly larger radius of curvature (94.99±13.34 mm, range: 56.88-123.13 mm) than females (87.54±14.51 mm, range: 60.09-139.85 mm); the difference between genders being 7.45 mm ($p<.008$) (Table 3). Differences were also observed between studied sides with left IM canals having a larger radius of curvature (93.62±14.07 mm, range: 73.21-139.52 mm) than the right side (88.86±14.42 mm, range: 56.88-

123.13 mm), however this difference of 4.76 mm was not significant (p=.089) (Table 2). In combined comparison with gender and side, differences in radius of medial curvature were seen as well. The medial radius of curvature in males was on average 96.65±11.06 mm for the left-sided IM canals, and 93.63±15.03 mm for the right-sided (p=.428). For females, the left side radius of medial curvature was 91.13±15.90 mm and the right side was 83.51±11.82 mm (p=.053) (Table 3).

- Lateral segment: The mean radius of curvature for all subjects was 32.53±11.10 mm (range: 10.44-75.93 mm, Table 2). The average radius of curvature on the lateral side was larger in females (33.35±12.31 mm, range: 10.44-75.93 mm) than males (31.69±9.73 mm, range: 12.65-59.67 mm), but the results were not statistically significant (p=.463) (Table 3). Side effect was statistically non-significant as well, (p=.439) with left side mean radius of curvature being larger (left: 33.43±10.67 mm, range: 18.34-75.93 mm; right: 31.68±11.53 mm, range: 10.44-65.81 mm) (Table 2). Similarly, no significant difference was seen between genders when side was accounted. For females (left: 34.68±12.57 mm; right: 31.86±12.08 mm) and males (left: 31.90±7.77 mm; right: 31.51±11.23 mm) (Table 3). Finally, there was no significant correlation between medial and lateral radii of curvature (Pearson correlation coefficient -0.008, p=.934).

3.3.4 Absolute and True Clavicle Length

Overall, absolute length of the clavicles ranged between 125.24 – 176.46 mm in the population. An average clavicle was 151.76±11.66 mm long (Table 4). The absolute length of male clavicles was 159.97±8.52 mm, and the length of female clavicles was 143.86±8.35 mm. Males were significantly longer than females (p<.0001) (Table 5). Furthermore, the right-sided clavicles

(150.59±11.16 mm) were on average shorter than the left-sided ones (152.98±12.15 mm), with a difference of 2.39 mm, but it was not significant (p=.297) (Table 4). When grouping for both

Table 2 Radius of curvature and standard deviation of the IM canal in right and left-sided clavicles

	Radius of Curvature (mm) ± SD		
	Right	**Left**	**Overall**
Medial	**88.86 ± 14.42**	**93.62 ± 14.07**	**91.19 ± 14.38**
Lateral	**31.68 ± 11.53**	**33.34 ± 10.67**	**32.53 ± 11.10**

Table 3 Radius of curvature and standard deviation of the IM canal when grouped for gender, and when grouped for gender and anatomical side.

	Radius of Curvature (mm) ± SD			
	Females - Right	**Females - Left**	**Females**	**Overall**
Medial	**83.51 ± 11.82**	**91.13 ± 15.90**	**87.54 ± 14.51**	**91.21 ± 14.4**
Lateral	**31.86 ± 12.08**	**34.68 ± 12.57**	**33.35 ± 12.31**	**32.51 ± 11.1**
	Males - Right	**Males - Left**	**Males**	**Overall**
Medial	**93.63 ± 15.03**	**96.65 ± 11.06**	**94.99 ± 13.34**	**91.21 ± 14.4**
Lateral	**31.51 ± 11.23**	**31.90 ± 7.77**	**31.69 ± 9.73**	**32.51 ± 11.1**

gender and side, the left-sided male population had an absolute clavicle length of 162.64±8.15 mm, while right-sided males had an absolute length of 157.78±8.31 mm. This difference of 4.86 mm was significant (p=.041) (Table 5). In females the absolute length of left-sided clavicles was longer at 145.05±8.63 mm, while right-sided clavicles were 142.53±8.00 mm. However, with a difference of 2.52 mm it was not statistically significant (p=.277) (Table 5).

Table 4 Absolute and true length of the clavicle when grouped by anatomical side.

	Clavicle Length (mm) ± SD		
	Right	**Left**	**Overall**
Absolute	**150.59 ± 11.16**	**152.98 ± 12.15**	**151.76 ± 11.66**
True	**165.87 ± 12.23**	**167.41 ± 12.95**	**166.62 ± 12.55**

Table 5 Absolute and true length of the clavicle when grouped by gender and anatomical side

	Clavicle Length (mm) ± SD			
	Females - Right	**Females - Left**	**Females**	**Overall**
Absolute	**142.53 ± 8.00**	**145.05 ± 8.63**	**143.86 ± 8.35**	**151.76 ± 11.66**
True	**157.24 ± 9.15**	**158.81 ± 8.76**	**158.07 ± 8.89**	**166.62 ± 12.55**

	Males - Right	**Males - Left**	**Males**	**Overall**
Absolute	**157.78 ± 8.31**	**162.64 ± 8.15**	**159.97 ± 8.52**	**151.76 ± 11.66**
True	**173.56 ± 9.15**	**177.88 ± 8.85**	**175.51 ± 9.18**	**166.62 ± 12.55**

The mean true length was 166.62±12.55 mm with a range of 137.09-197.70 mm for the general population. Males had significantly longer clavicles ($p<.0001$) than females with an average size for males 175.51±9.18 mm and females 158.07±8.89 mm (Table 5). Overall, anatomical side did not influence true length either ($p=.533$). Right-sided clavicles (165.87±12.23 mm) and the left-sided (167.41±12.95 mm) only differed by 1.54 mm (Table 4). Likewise, the side differences were not significantly different within the male population (left: 177.88±8.85 mm; right: 173.56±9.15 mm; difference: 4.32 mm; $p=.094$) and female population (left: 158.81±8.76 mm; right: 157.24±9.15 mm; difference: 1.57 mm; $p=.528$).

The difference in length between absolute and true length measurements was on average 14.86 mm. The measure of true length of the clavicle was significantly larger than the measure of absolute clavicle length in the general population, as well as within each gender and side ($p<.0001$). Clavicle true and absolute length were highly correlated (Pearson correlation coefficient 0.964, $p<.0001$; Figure 14.

CHAPTER 4: DISCUSSION

4.1 Results Comparison with Previous Literature

Refer to Appendix A. for a direct comparison between results from selected previous studies and results of this study.

The most influential clavicle morphometry study was done by Andermahr et al. [8]. Their work was one of the first to address IM canal dimensions and have been the most cited in later publications. Instead of using CT scans, cadaveric clavicles were cut using a saw at angles perpendicular to the curvature of the bone at many locations (15%, 25%, 33%, 50%, 66%, 75%, and 85% clavicle length). Even though these angles were estimated by the operator, this method ensured that the cross-sections obtained were true to the clavicle's geometry and not to the orientation of the body within a CT scanner. Another feature of this study was the inclusion of anatomically relevant zones (superior, inferior, anterior and posterior) for each cross-section, and taking two measurements in this plane perpendicular to each other. In the end, these two IM canal diameters were averaged. A summary of their IM canal results can be seen in Table A.3. The largest difference between the IM diameter in the study by Andermahr et al. and the current study is seen at 15% and 85% clavicle length (medial and lateral ends respectively). The difference was 8 mm, with the current study data being the smaller of the two (medial: 18 mm - 10 mm, lateral 15 mm - 7 mm). However, this difference becomes smaller, 2 mm, within the mid-third of the clavicle (7 mm - 5mm at 50% and 8 mm - 6 mm at 66%). This pattern is due to the key

differences in methodology between studies. While Andermahr et al. measured independent IM canal diameters for each cross-section, the current study's IM diameters had to be bounded within the inscribed circle inside the canal. Because the clavicle tends to deviate from a circular cross-sectional shape towards its medial and lateral ends, this discrepancy in results becomes obvious in these locations (Figure 23).

The next studies that addressed IM canal diameter were Mathieu et al. [9] and King et al. [11]. Their work focused on expanding the literature on IM canal parameters by grouping for gender to ascertain differences due to sexual dimorphism, as well as to investigate differences due to anatomical side. King et al. had a very large sample size of 418 clavicle CT scans, and an operator measured the IM canal in the axial CT plane using the PACS radiology system. Their results were very close in value to the current study's results, and these similarities were consistent throughout the length of the clavicle. Also, similar to Andermahr et al., the results from King et al. were greater than the current study due to the same differences in methodology (simple line diameter vs. inscribed circle diameter) (Table A.3). King et al. female and male IM diameter at 17% clavicle length averaged 8.5 mm and 10.0 mm respectively, while the current study averaged 7.9 mm and 10.4 mm respectively. Furthermore, King et al. female and male IM diameter at 50% clavicle length averaged 5.5 mm and 6.8 mm, while the current study averaged 3.9 and 5.2 mm respectively. For the same reasons described above regarding differences in methodology (Figure 23), the results from the study by Mathieu at al. also tend to be larger than the current study results, especially on the medial and lateral ends. Their female and male IM diameter at 15% clavicle length averaged 15.2 mm and 19.4 mm respectively, while the current study averaged 8.8 and 11.3 mm respectively. In addition, female and male IM diameter at 50%

clavicle length averaged 5.5 mm and 6.8 mm, while the current study averaged 3.9 mm and 5.2 mm respectively (Table A.3).

Eight studies addressed clavicle cross-section diameter at locations along the clavicle that were comparable to the current study. Contrary to the patterns seen in IM canal results, all of these studies measured a slightly smaller (on the order of 2 mm difference) clavicle diameter. Out of the eight, the one that obtained the most complete representation of clavicle parameters along its length was done by Daruwalla et al. [16]. Their very thorough and detailed methods describe their acquisition of a 3D coordinate system for each clavicle. They selected multiple points on the flat lateral surface of the clavicle to create a best fit transverse plane. Within this plane, a line connecting both ends of the clavicle was created. Consequently, the clavicle was cut into 50 slices perpendicular to this connecting line, and the height and width of each slice was measured. Starting at 10%, clavicle diameter in females was 15.5 x 19.6 mm compared to 22.9 in the current study, and in males was 17.3 x 19.3 mm compared to 26.6 mm. This difference becomes smaller as the center of the clavicle is approached. In females it was 9.6 x 9.3 mm compared to 12.0 mm in the current study, and in males was 12.8 x 11.7 mm compared to 15.6 mm. Because the circumscribed circles enclose the bone in its entirety, their diameters represent the largest clavicle diameter possible at any given cross-section. Figure 23 illustrates the differences between methodologies used. Thus, any other clavicle diameter within the same cross-section will be either equal to or less than the circumscribed circle diameter.

Another noteworthy study, by Bernat et al. [12], used cylinder parameterization to quantify clavicle geometry. However, instead of reporting the clavicle cross-section height and width at pre-determined locations along its length, they divided the bone into medial and lateral

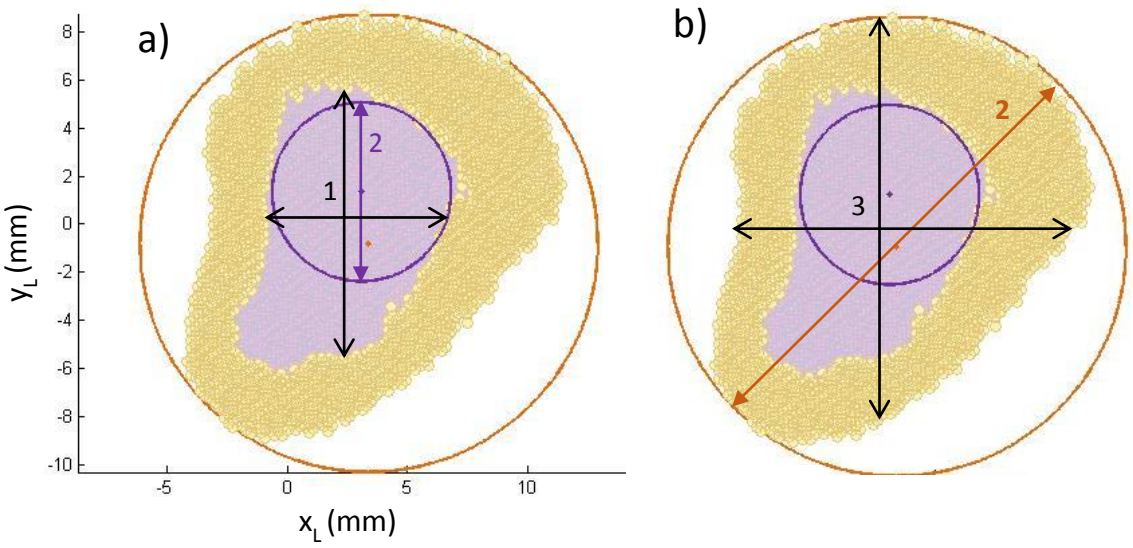

Figure 23 Differences in a) IM canal diameter measurements of a lateral-end slice and b) clavicle diameter measurements when comparing multiple studies. 1- Andermahr et al. [8] 2- Current study. 3- Daruwalla et al. [16].

halves and sought the value of the largest height and width of that region, and reported the location where it was found. Moreover, they reported the smallest height and width of the entire clavicle in a similar fashion. These results are summarized in Table A.2. Within the medial section, Bernat et al. located the greatest clavicle width (23.8 mm) at 4.8% length and greatest height (25.6 mm) at 4.9%, while the current study found the greatest clavicle diameter (29.1 mm) at 5% length. Due to the tightest-fit box being cut into 100 sections, each one representing 1% clavicle length, it is not feasible to find parameters with an accuracy finer than 1%. This means a maximum diameter found at 4.9% could very well fall into the 5% slice of the current study. The rest of the locations of maximum clavicle diameter are very similar, with only discrepancies between 0-1%. It is also important to note the differences in diameter values ranging from 7 mm to 1 mm. Similar to Daruwalla et al., Bernat et al. also took simple linear measurements of clavicle

height and width, and thus their values are also smaller than the current study values, which represent the largest clavicle cross-section (Table A.2) (Figure 23). Again, this difference becomes more pronounced towards the medial and lateral ends of the clavicle.

Radius of curvature of the IM canal has not been measured before. Previous studies, such as king et al. [11], Bachoura et al. [13], and Daruwalla et al. [16] have only sought the IM canal angle of curvature by estimating straight lines through the center of the 3 sections (lateral, middle and medial) and measuring the angle between these lines. Even Bernat et al., who used a true clavicle centerline, did not find its radius of curvature. However, the IM canal radius of curvature found in the current study can be compared to the outer clavicle radius of curvature and note the similarities between these two parameters. Mathieu et al. [9], Bachoura et al. [13], (13) Andermahr et al. [8], and Duprey et al. [17] measured the medial radius of curvature of the outer cortex (Figure A.2), and all were consistently smaller (range of difference: 10 – 29 mm) than the IM radius of curvature measured in this study. On the other hand, lateral radius of curvature from the studies by Matieu et al., Bachoura et al., and Andermahr et al. were larger (range of difference: 2 mm – 7 mm), and only Duprey et al. had a smaller lateral radius of curvature (difference: 5 mm).

A total of nine studies examined clavicle lengths, but only two, King et al. and Bernat et al., used true clavicle length. The reported true length for all subjects from Bernat et al. was 160 mm while from the current study was 166 mm. Differences in such results could be attributed to differences between cylinder parameterization and circumscribed circle calculation The results from King et al. (151 mm) were much shorter because they used three straight lines to calculate true clavicle length (Table A.5). The rest of the studies that only addressed absolute clavicle

length were fairly similar to the current results, with the exception of both studies by Bachoura et al. [46] [13] (137 mm and 136 mm vs. current study of 152 mm.) (Table A.5).

Finally, IM canal and clavicle center displacement cannot be compared to any previous studies. Since the publication of the work by Andermahr et al., it seems that many have followed their steps in finding depth of curvature. These two parameters, while similar, share noteworthy differences that prevent them from being comparable. First, depth of medial curvature is a measurement that starts from an axis along the maximum lateral curvature, and 2) it ends at a maximized distance on the outside medial curvature cortex (Figure A.2). On the other hand, center displacement is a measurement that starts on the 'z_L' axis and ends at the center of the cross-section.

4.2 Implications of Study

The aims of this study were to 1) quantify clavicle and IM canal dimensions and geometry using a 3D model, and 2) evaluate the effect of gender and anatomical side on the morphometric parameters of the human clavicle and IM canal.

Firstly, clavicle length is a parameter that is often underestimated. Because of its signature S-shape, the dimensions of the bone are misrepresented. Instead, true clavicle length offers a better representation, as it is the actual length of the clavicle if it were straight. On average right-sided clavicles tend to be shorter than their left counterparts, but this finding is not always significant [8] [12] [16] [14] (Table 4). However, males are significantly longer than females, both in absolute and true length (Table 5). To an extent, the difference between absolute and true clavicle lengths can provide some insight into the amount of curvature present,

because these parameters are highly correlated. Thus, if a clavicle becomes longer, so will the length of the curvature by a proportional amount.

Secondly, a better method of quantifying the S-shape of the clavicle is finding the radius of curvature of the IM canal. Males have significantly greater medial curvatures than females and this is most likely due to their greater size. Similarly, left-sided clavicles tend to be longer and have a greater medial curvature, but it is not statistically significant. On the other hand, it seems that lateral curvature is not affected by either gender or anatomical side. Longer clavicles do not necessarily confer larger radii of curvature, and both medial and lateral radii of curvature are not correlated to one another. In addition, IM canal radius of curvature, especially the medial one, represents the safest trajectory an IM device would take as it is being inserted into the canal, and also is the curvature this device should have in order to fit properly inside. This is because the medial radius of curvature (from 15-63%) covers the location where the most frequent clavicle fractures occur (mid-shaft: 33-66%).

Thirdly, the diameter of circumscribed circles represent the largest clavicle diameter at any given cross-section. When this parameter is examined along the entire clavicle length, it always exhibits a minimum near the half-way point. The value of this diameter at the narrowest region is statistically significant for gender. Overall, males have thicker clavicles than females; this finding was also true with previous studies [12]. While right-sided clavicles tend to be thicker than right-sided ones [14], this finding was not statistically significant. The IM canal also exhibits a minimum near the half-way point. However, these narrowing regions were observed at different locations along the clavicle (Figures 15-18). These differences were observed across all groups (male/female, right/left), but showed no obvious trend among them. Overall, the

different locations of narrowing between clavicle and IM canal occurred over a 5% clavicle length; this suggests that, on average, one may not estimate the location of the narrowest region of the IM canal, based on external visualization of the clavicle alone. The narrowing of the IM canal is of special interest because this is the limiting region for an IM device. Given the signature hourglass-shape of the IM canal volume (figure 4 d), if an IM device is fabricated to pass safely through this problematic region, it will fit properly inside the rest of the canal. Furthermore, both the clavicle and IM canal narrowing regions play an important role in mid-shaft clavicle fracture patterns. When starting at the medial end, the clavicle narrows before the IM canal. This could imply a local thinning of the cortical bone which could very well explain why the most type of clavicle fractures occur in this region.

Lastly, the center of circumscribed circles follow the clavicle's signature S-shape, with maximum displacements from the longitudinal axis 'z_L' in halfway through each curve (medial and lateral), and an inflection point at 63% length. The values of maximum displacement were statistically significant for gender; males exhibited deeper curves. This means that not only are male clavicles longer than females, but they are larger overall; the S-shape is conserved regardless of size, as the bone is scaled proportionally larger for males. There is no significant difference of maximum displacement between left and right-sided clavicles. Similar to circumscribed circles, the centers of inscribed circles are displaced the furthest halfway through each curve (medial and lateral). However, the location and value of maximum displacement is different compared to the circumscribed circles, especially in the lateral curvature (Figures 19-21). This implies there exists an eccentricity of the IM canal center with respect to the clavicle center in the 'y_L' axis. This eccentricity or difference between circumscribed and inscribed circles

could infer asymmetrical differences in cortex thickening within a given cross-section. This is understandable for cross-sectional areas that are near circular, but may signify something different is occurring in the far lateral end of the clavicle. Circle eccentricity may actually be due an irregular shape in the cortex's cross-section; the inscribed circle is "pushed" towards the wider area in the canal as the cross-section takes on a more triangular shape. In these instances, the eccentricity would tell us how close the device can be to the outer surface of the bone, not so much on how thick the cortex actually is along a specific axis (Figure 24).

4.3 Study Limitations

This study has several limitations:

- The population used in this study does not represent healthy individuals, rather patients with upper extremity related issues. This is a retrospective study on the patients who underwent shoulder arthroplasty due to progressive joint disease or cuff tear. Although the studied bones were examined for abnormalities and congenital malformations, the studied bone structures could carry underlying changes in shape caused by shoulder pathology. In addition, the age distribution of subjects enrolled in this study was affected by the fact that occurrence of upper extremity pathology that leads to shoulder arthroplasty is very specific (65.4±11.0 years) and under no circumstances can be considered normal (including evenly younger and older individuals). This fact should be taken into consideration when results are interpreted as morphological and morphometric characteristics of bone can be significantly affected by age and combined effect of age and gender. In addition, because common shoulder problems such as osteoarthritis and rotator cuff tear occur in the elderly population, the population in this study was also old (range: 33 – 86 years, mean: 65.4±11.0 years).

- The segmentation process, creating surface and volumetric models, is not an automated process. Thus the potential for operator-induced error and discrepancies from model to model can occur. This error can be significantly reduced when only one operator following a standardized protocol creates all the models (previous study found little discrepancy in operator error [14]). In this study, all models were created following standardized protocol by a single operator.

- Furthermore, the orientation of the patient in the CT scanner limits the resolution of the clavicle. Ideally, an object should be scanned longitudinally, with the CT slices perpendicular to this axis. Because the clavicle is oriented in a medial-lateral direction within the body, and the subject is positioned superior-inferiorly into the machine, it is not possible for the CT to slice the image of the clavicle in this fashion.

- Application of the principal component analysis works well for the majority of clavicles (due to its signature S-shape), but can be problematic for a small group of individuals with a dominant inferior curvature of the clavicle in the '$[x_L,z_L]$' plane (2/104 patients in our study group), over the medial/lateral curves, in the '$[y_L,z_L]$' plane. In these cases, because clavicle voxels exhibited more variation in the 'x_L' direction than in the 'y_L' direction, these would become the second and third components respectively. Thus, the second and third components would have to swap places to revert the clavicle to the proper orientation with respect to the rest of the population.

- In ideal solution, the inflection point of the IM canal would be ascertained from finding where the second derivative of the function given by the IM canal centerline $\mathbf{CL_i}$ equals 0. To do this, one would have to approximate $\mathbf{CL_i}$ as a higher order polynomial function. The above

described approach was not efficient for our analysis. A fitted polynomial does not yield an optimal (anatomically relevant) solution. Instead, in our approach the inflection point was estimated by finding the point along $\mathbf{CL_i}$ that crosses the longitudinal axis 'z_L'. This was at approximately 62% clavicle length from the medial end in most cases (Figure 19).

- Circumscribed circles measure the largest diameter of any given clavicle cross-section. The approximation of clavicle diameter using these circles works well when the cross-sectional shape is near circular, but becomes less accurate as the clavicle takes on a different shape. This occurs towards the lateral end of the clavicle, where it flattens. Furthermore, the deviation from a circular shape affects the positioning of the inscribed circle relative to the circumscribed one. Thus, the noted eccentricity that occurs in this region does not tell us much about cortical thickness, but may explain changes in cross-sectional shape to a more asymmetrical one (Figure 24).

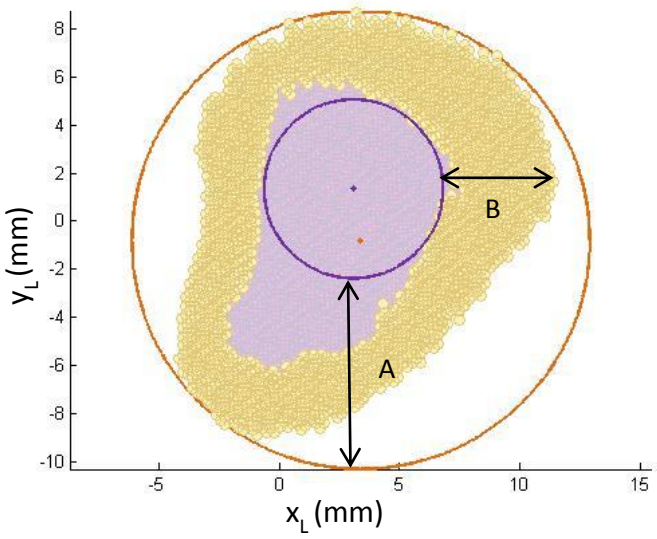

Figure 24 Example slice taken near the lateral end of the clavicle. Line A shows the difference between circumscribed and inscribed circle displacement, while line B shows the thickest cortex region. Note the eccentricity between inscribed and circumscribed circle centers.

- While Inscribed circles are useful for estimating the largest diameter an IM device with a circular cross-section can be, it does not provide information on the single largest distance between cortical walls in the canal. In addition, although the cross-section of the IM canal is mostly circular, it also tends to change shape towards the lateral end of the clavicle (Figure 24). Thus, inscribed circles are not ideal in describing IM canal shape changes that occur along its lateral end, nor should it be used in conjunction with circumscribed circles to estimate cortical thickness.

CHAPTER 5: CONCLUSION

5.1 Innovation of Study

The aim of this study was to quantify 3D morphometry of the clavicle and its IM canal, namely size (length, width, depth), radius of curvature, and clavicle and IM canal diameter as a function of length. Despite the existence of previously published work on clavicle morphometry, the aim was to offer a more accurate description of the above mentioned parameters. Previous works provide significant volume of data on the clavicular morphometry as well as some basic data on the IM canal, however, after rigorous literature review the true 3D data on clavicular morphometry and parametrization of the IM canal in particular were lacking.

The most important difference between this study and numerous previous studies is the true 3D nature of the utilized methodology. The current approach, in contrast, was free of subject-specific bias introduced by the initial position and orientation of the patient during the CT scanning (orientation of the slices); instead, all measurements taken were established on the individual clavicle geometry.

A second noteworthy difference of this study is its methodological automatic design. This approach aids in removing biases that are often induced by the methods and observers. The fully automated process starts once the volumetric and surface models are obtained (flowchart/diagram of this) and removes manual error and operator-induced subjectivity at every step of the process (Figure 25). The removal of error at each step prevents it from amplifying in

downstream calculations from the initial point. Additionally, this approach does not allow anatomically relevant point selection (by observer) in defining anatomical references or performing measurements by point selection.

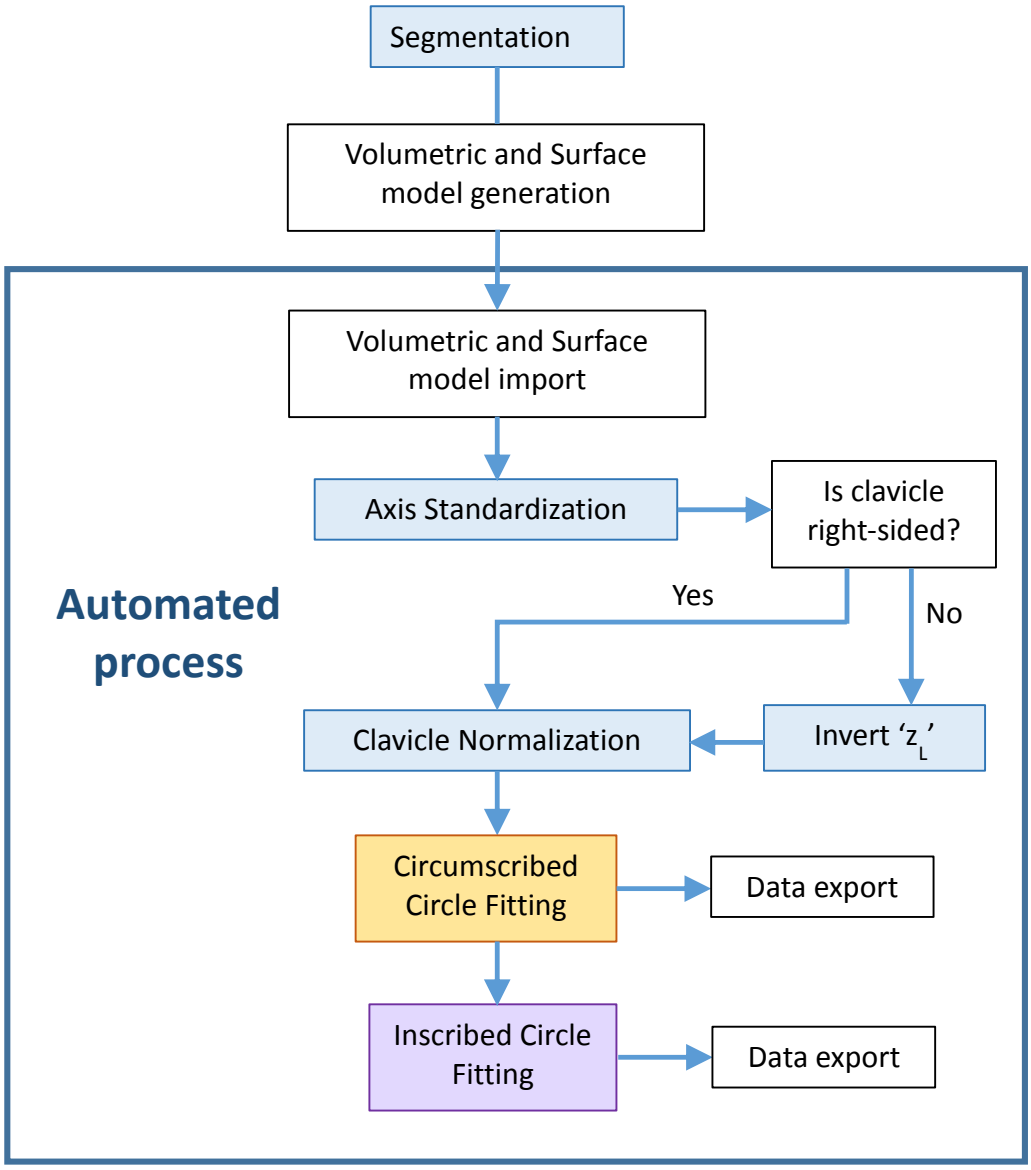

Figure 25 Diagram depicting a summary of methods and indicating the automated portion of the process.

And finally, this work looks at the 3D parametrization of the IM canal, as well as its relationship to the clavicle and patient specifics (gender and side). Up to our best knowledge, this

is the only published study to report on IM canal parameters in 3D. Radius of curvature of the IM canal has not been reported before. This parameter, along with the measurement of the IM canal diameter and the location of its narrowest region will aid in the design of IM devices for mid-shaft clavicle fixation.

5.2 Contributions to the Field

The most significant contribution of this work to the pool of scientific knowledge is the detailed 3D description of the clavicle IM canal geometry and its relationship to the clavicle as a whole. Moreover, data on clavicular morphometry is measured using a refined methodology of increasing accuracy and repeatability. This work is multidisciplinary in nature, and as such can contribute to different fields: basic science, implant design, and clinical practice.

Firstly, the results of this work would be beneficial to increase the knowledge of basic characteristics of the clavicular anatomy. The increase in accuracy and normalization of the study population can serve as a useful baseline for understanding the functional anatomy of the clavicle and its pathological changes. Alteration in size and shape of the clavicle as well as differences in cortical thickness (estimated by subtracting inscribed circle from circumscribed circle) can be explained by alterations in muscles attached to the clavicle. Proper interpretation of the results of this study can offer insight into those often complex interactions. While this was not the intent of this study, the methods developed are flexible to be adapted for other future basic science research endeavors.

Secondly, this study provides an unbiased representation of clavicle spatial geometry. Based on this data, parametric models of an average clavicle can be made for each gender/side. This model can be further utilized by engineers in R&D during implant design and testing. Based

on the data, several sizes of the implant would be necessary. The primary parameter to consider for the device design would be the IM canal radius with a maximum of 2.5 mm for males, and 1.9 mm for females. The secondary parameter to be considered for implant design would be the implant curvature. Appropriate mechanical testing of the potential implant would have to be performed. However, based on the results of this study one can speculate that the IM device may serve as a viable alternative to external plate fixation of mid-shaft clavicle fractures, as IM canal and its curvature does not prevent device fit. Since 3D morphometric analysis is a requisite for noting the different locations of clavicle and IM canal narrowing, a pre-operative CT scan and canal analysis would be warranted in pre-operative planning and implant selection for fracture treatment with an IM device

Thirdly, the contribution to the clinical practice. It is a common practice to evaluate the severity of mid-shaft clavicle fractures using conventional radiographs (Figure 2). The amount of overlap between both bone segments, as a measure of severity and primary diagnostic tool in decision making between conservative and surgical treatment, is measured on a 2D X-ray. Traditionally, if it is greater than 2 cm, the degree of displacement is considered severe and the clinician may opt for surgical approach. Our data suggest that there is a difference between true (as a length measured on a 3D curve) and absolute (can be approximated as a 2D length in frontal plane) clavicle lengths. Because true length of the clavicle is a superior estimation of its length than the absolute, there may be a longer region of overlap not appreciable on X-ray. In reality, one can speculate that the 2 cm rule of thumb may be underestimating displacement severity. Clinically, the loss of clavicular length can have severe long-term consequences as the clavicle is an equally important member of the complex humero-scapular-thoracic structure. Significant

shortening of the clavicle can alter these relationships and can lead to changes in arm range of motion, patterns of motion (humerus, scapula and spine all move in rhythm), increase joint stiffness, and an influence on the pathological processes (such as osteoarthritis, cuff tear, etc.).

5.3 Future Work

Firstly, additional parameters relating to clavicle morphometry need to be explored. The most important one that has not been fully addressed yet is cortex thickness. While there is indirect information describing the cortex's potential variation in thickness (inscribed circle diameter subtracted from circumscribed circle diameter), it is not an accurate depiction of reality. Further code is in progress that will use the Hounsfield unit value for each voxel in a cross-section to determine the boundaries of cortical bone between IM canal and soft tissue. Consequently, the algorithm would use the geometric center of each cross-section and measure cortex thickness in a radially outward direction. This can be done for each anatomically relevant zone (anterior, posterior, superior and inferior) (Figure 26). Cortex thickness data would be of interest to investigate possible relationships between bone thickness and other clavicle parameters such as clavicle length, curvature and cross-sectional diameter, and between patient information such as age, gender, hand-dominance, height and weight.

Furthermore, Hounsfield unit values can be used to investigate bone density distribution in the clavicle. High and low dense bone tissue areas can be analyzed as a function of clavicle length (Figure 27). The boundaries between these high and low density areas could have potential applications in the influence of clavicle fracture patterns. This could be accomplished by establishing approximate fracture locations on diagnostic film and finding any correlations

with bone density distribution and bone narrowing regions. In addition, understanding bone density distribution could aid in the planning of nail and screw positioning.

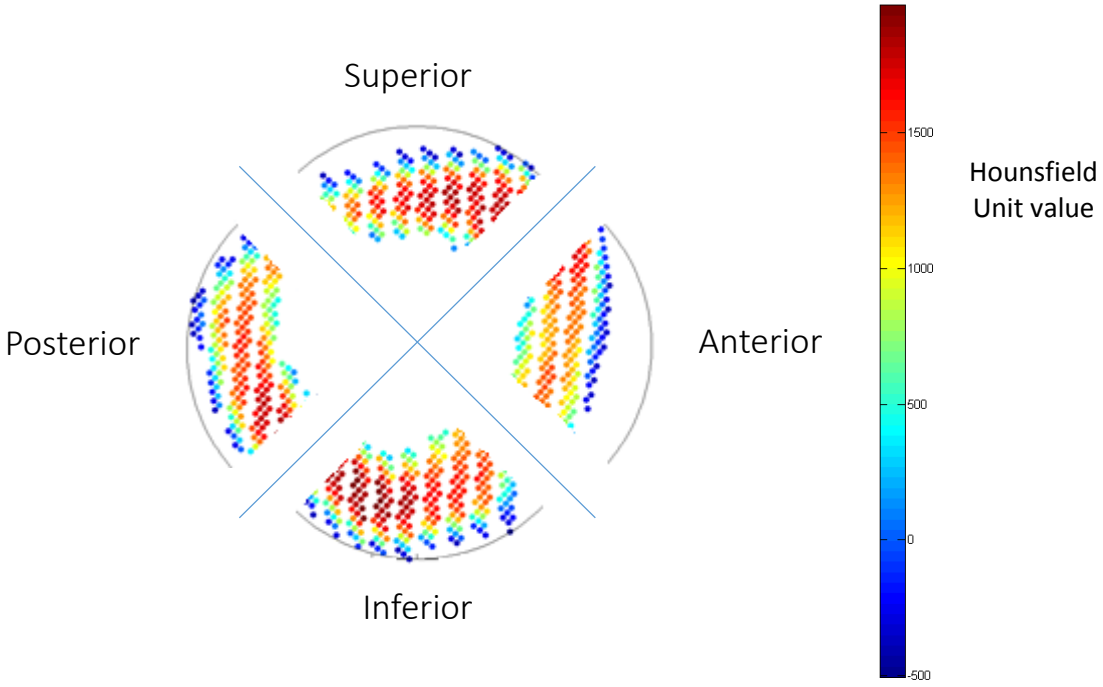

Figure 26 Future work depicting a potential method of zoning and calculating clavicle cortex thickness at a particular cross-section.

Another topic for the future would be improving the method of normalization. Currently, the tightest-fit box is cut into slices that are all perpendicular to the main axis 'z_L'. However, a more accurate representation of cross-sectional geometry should be obtained from a plane that is instead perpendicular to the clavicle centerline. This is the same line that is used to measure true clavicle length. As a result, the orientation of these slices will twist along the length of the clavicle to accommodate its signature S-shape (Figure 28).

In addition to adding more clavicle parameters, the population should be expanded. In the study limitations, a lack of healthy and young individuals was noted. Thus, to further the

literature on human clavicle morphometry, a large sample population that better represents the true population distribution in terms of age and health status is essential.

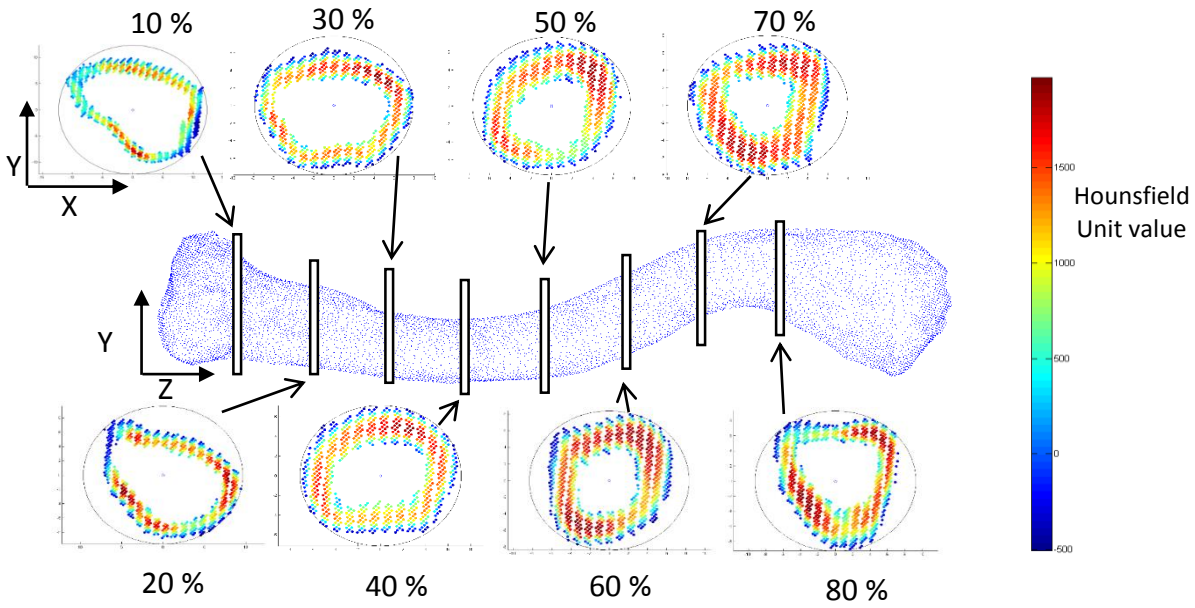

Figure 27 Future work depicting the potential analysis of cortical bone density distribution as a function of clavicle length.

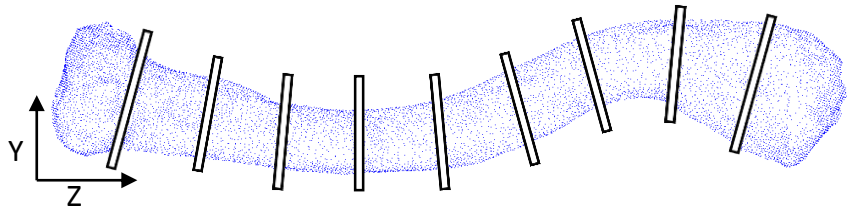

Figure 28 Future work depicting clavicle cross-section slices taken perpendicular to the centerline. For simplicity, only 9 slices are shown.

Lastly, a logical next step in this research would be to test IM devices fabricated to match the parameters in this study. Using a statistical approach, the data grouped for gender and anatomical side can be used to find optimal IM device dimensions for various sizes (small, medium and large) for each subpopulation. Each size could then be mechanically tested in

cadaveric clavicles against anterior and superior plating to find the optimal mid-shaft clavicle fracture treatment. Due to the small size of IM canals and narrowing seen in females, an IM device with a cross-sectional radius of 1.9 mm could potentially be unfeasible, and it would be important for a clinician to understand this if his/her patient falls in this category, and explore other options.

REFERENCES

1. Postacchini, F., et al., *Epidemiology of clavicle fractures.* J Shoulder Elbow Surg, 2002. **11**(5): p. 452-6.

2. Paladini, P., et al., *Treatment of clavicle fractures.* Transl Med UniSa, 2012. **2**: p. 47-58.

3. Lenza, M. and F. Faloppa, *Surgical interventions for treating acute fractures or non-union of the middle third of the clavicle.* Cochrane Database Syst Rev, 2015. **5**: p. CD007428.

4. Shah, A.S., et al., *Stabilization of adolescent both-bone forearm fractures: a comparison of intramedullary nailing versus open reduction and internal fixation.* J Orthop Trauma, 2010. **24**(7): p. 440-7.

5. Duan, X., et al., *Plating versus intramedullary pin or conservative treatment for midshaft fracture of clavicle: a meta-analysis of randomized controlled trials.* J Shoulder Elbow Surg, 2011. **20**(6): p. 1008-15.

6. Zhang, B., et al., *Meta-analysis of plate fixation versus intramedullary fixation for the treatment of mid-shaft clavicle fractures.* Scand J Trauma Resusc Emerg Med, 2015. **23**: p. 27.

7. Barlow, T., J. Beazley, and D. Barlow, *A systematic review of plate versus intramedullary fixation in the treatment of midshaft clavicle fractures.* Scott Med J, 2013. **58**(3): p. 163-7.

8. Andermahr, J., et al., *Anatomy of the clavicle and the intramedullary nailing of midclavicular fractures.* Clin Anat, 2007. **20**(1): p. 48-56.

9. Mathieu, P.A., et al., *Anatomical study of the clavicle: endomedullary morphology.* Surg Radiol Anat, 2014. **36**(1): p. 11-5.

10. Nourissat, G., et al., *Three-dimensional computed tomographic scan of the external third of the clavicle.* Arthroscopy, 2007. **23**(1): p. 29-33.

11. King, P.R., S. Scheepers, and A. Ikram, *Anatomy of the clavicle and its medullary canal: a computed tomography study.* Eur J Orthop Surg Traumatol, 2014. **24**(1): p. 37-42.

12. Bernat, A., et al., *The anatomy of the clavicle: a three-dimensional cadaveric study.* Clin Anat, 2014. **27**(5): p. 712-23.

13. Bachoura, A., et al., *Clavicle morphometry revisited: a 3-dimensional study with relevance to operative fixation.* J Shoulder Elbow Surg, 2013. **22**(1): p. e15-21.

14. Abdel Fatah, E.E., et al., *A three-dimensional analysis of bilateral directional asymmetry in the human clavicle.* Am J Phys Anthropol, 2012. **149**(4): p. 547-59.

15. Daruwalla, Z.J., et al., *An application of principal component analysis to the clavicle and clavicle fixation devices.* J Orthop Surg Res, 2010. **5**: p. 21.

16. Daruwalla, Z.J., et al., *Anatomic variation of the clavicle: A novel three-dimensional study.* Clin Anat, 2010. **23**(2): p. 199-209.

17. Duprey, S., K. Bruyere, and J.P. Verriest, *Influence of geometrical personalization on the simulation of clavicle fractures.* J Biomech, 2008. **41**(1): p. 200-7.

18. Moore, K.L. and A.F. Dalley, *Clinically oriented anatomy*. Fith ed. 2006, Baltimore: Lippincot Williams & Wilkins. 1209.

19. Schwarzkopf, R., et al., *Distal clavicular osteolysis: a review of the literature.* Bull NYU Hosp Jt Dis, 2008. **66**(2): p. 94-101.

20. Moonot, P. and N. Ashwood, *Clavicle fractures.* Trauma, 2009. **11**(2): p. 123-132.

21. Galley, I.J., A.C. Watts, and G.I. Bain, *The anatomic relationship of the axillary artery and vein to the clavicle: a cadaveric study.* J Shoulder Elbow Surg, 2009. **18**(5): p. e21-5.

22. Lu, Y.C. and C.D. Untaroiu, *Statistical shape analysis of clavicular cortical bone with applications to the development of mean and boundary shape models.* Comput Methods Programs Biomed, 2013. **111**(3): p. 613-28.

23. Gumustekin, K., et al., *Handedness and bilateral femoral bone densities in men and women.* Int J Neurosci, 2004. **114**(12): p. 1533-47.

24. Walters, J., et al., *Effect of hand dominance on bone mass measurement in sedentary individuals.* J Clin Densitom, 1998. **1**(4): p. 359-67.

25. Teodoro Ezequiel Guerra, M., et al., *Densitometric study of the clavicle: bone mineral density explains the laterality of the fractures.* Rev Bras Ortop, 2014. **49**(5): p. 468-72.

26. Falys, C.G. and D. Prangle, *Estimating age of mature adults from the degeneration of the sternal end of the clavicle.* Am J Phys Anthropol, 2015. **156**(2): p. 203-14.

27. Van Tongel, A., I. Piepers, and L. De Wilde, *The significance of the clavicle on shoulder girdle function.* J Shoulder Elbow Surg, 2015. **24**(9): p. e255-9.

28. Matsumura, N., et al., *The function of the clavicle on scapular motion: a cadaveric study.* J Shoulder Elbow Surg, 2013. **22**(3): p. 333-9.

29. Sood, A., N. Wallwork, and G.I. Bain, *Clinical results of coracoacromial ligament transfer in acromioclavicular dislocations: A review of published literature.* Int J Shoulder Surg, 2008. **2**(1): p. 13-21.

30. Mall, N.A., et al., *Degenerative joint disease of the acromioclavicular joint: a review.* Am J Sports Med, 2013. **41**(11): p. 2684-92.

31. Patel, B., P.A. Gustafson, and J. Jastifer, *The effect of clavicle malunion on shoulder biomechanics; a computational study.* Clin Biomech (Bristol, Avon), 2012. **27**(5): p. 436-42.

32. Donnelly, T.D., et al., *Fractures of the clavicle: an overview.* Open Orthop J, 2013. **7**: p. 329-33.

33. Low, A.K., D.G. Duckworth, and D.J. Bokor, *Operative outcome of displaced medial-end clavicle fractures in adults.* J Shoulder Elbow Surg, 2008. **17**(5): p. 751-4.

34. Faraud, A., et al., *Outcomes from surgical treatment of middle-third clavicle fractures non-union in adults: a series of 21 cases.* Orthop Traumatol Surg Res, 2014. **100**(2): p. 171-6.

35. Zlowodzki, M., et al., *Treatment of acute midshaft clavicle fractures: systematic review of 2144 fractures: on behalf of the Evidence-Based Orthopaedic Trauma Working Group.* J Orthop Trauma, 2005. **19**(7): p. 504-7.

36. McKee, M.D., et al., *Deficits following nonoperative treatment of displaced midshaft clavicular fractures.* J Bone Joint Surg Am, 2006. **88**(1): p. 35-40.

37. Virtanen, K.J., et al., *Sling compared with plate osteosynthesis for treatment of displaced midshaft clavicular fractures: a randomized clinical trial.* J Bone Joint Surg Am, 2012. **94**(17): p. 1546-53.

38. *Nonunions*. OrthoInfo 2014 March 2014; Available from: http://orthoinfo.aaos.org/topic.cfm?topic=A00374.

39. Martetschläger, F., T.R. Gaskill, and P.J. Millett, *Management of clavicle nonunion and malunion.* J Shoulder Elbow Surg, 2013. **22**(6): p. 862-868.

40. Wang, X., et al., *Minimally invasive in the treatment of clavicle middle part fractures with locking reconstruction plate.* Int J Surg, 2014. **12**(7): p. 654-8.

41. Barlow, T., P. Upadhyay, and D. Barlow, *External fixators in the treatment of midshaft clavicle non-unions: a systematic review.* Eur J Orthop Surg Traumatol, 2014. **24**(2): p. 143-8.

42. Zehir, S., et al., *Comparison of novel intramedullary nailing with mini-invasive plating in surgical fixation of displaced midshaft clavicle fractures.* Arch Orthop Trauma Surg, 2015. **135**(3): p. 339-44.

43. Hulsmans, M.H., et al., *Anteroinferior versus superior plating of clavicular fractures.* J Shoulder Elbow Surg, 2015.

44. Gilde, A.K., et al., *Does plate type influence the clinical outcomes and implant removal in midclavicular fractures fixed with 2.7-mm anteroinferior plates? A retrospective cohort study*, in *Orthopaedic Surgery and Research*. 2014, BioMed Central Ltd.

45. Lai, Y.C., et al., *Comparison of dynamic and locked compression plates for treating midshaft clavicle fractures.* Orthopedics, 2012. **35**(5): p. e697-702.

46. Bachoura, A., A.S. Deane, and S. Kamineni, *Clavicle anatomy and the applicability of intramedullary midshaft fracture fixation.* J Shoulder Elbow Surg, 2012. **21**(10): p. 1384-90.

47. Golish, S.R., et al., *A biomechanical study of plate versus intramedullary devices for midshaft clavicle fixation.* J Orthop Surg Res, 2008. **3**: p. 28.

48. Figueiredo, G.S., et al., *Correlation of the degree of clavicle shortening after non-surgical treatment of midshaft fractures with upper limb function.* BMC Musculoskelet Disord, 2015. **16**: p. 151.

49. Nicoguaro. *PCA of a multivariate Gaussian distribution*. 2016; Available from: https://commons.wikimedia.org/wiki/File:GaussianScatterPCA.svg.

APPENDIX A: RESULTS COMPARISON WITH PREVIOUS STUDIES

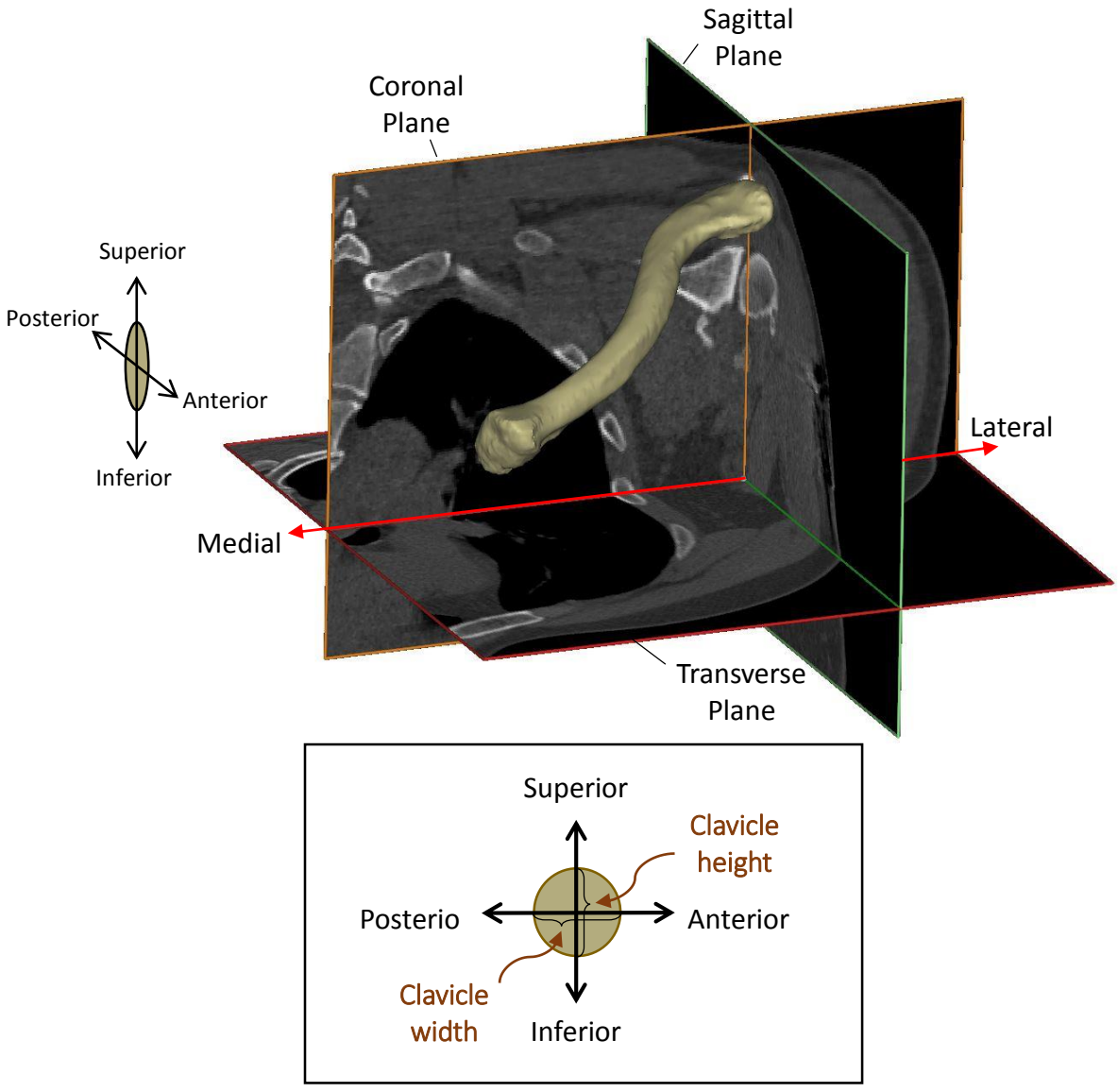

Figure A.1 Clavicle height and width in reference to its anatomy. Some authors reported their results as “height and width” while others used anatomical directions. Height corresponds to a measurement in the superior-inferior direction, while width corresponds to a measurement in the anterior-posterior direction.

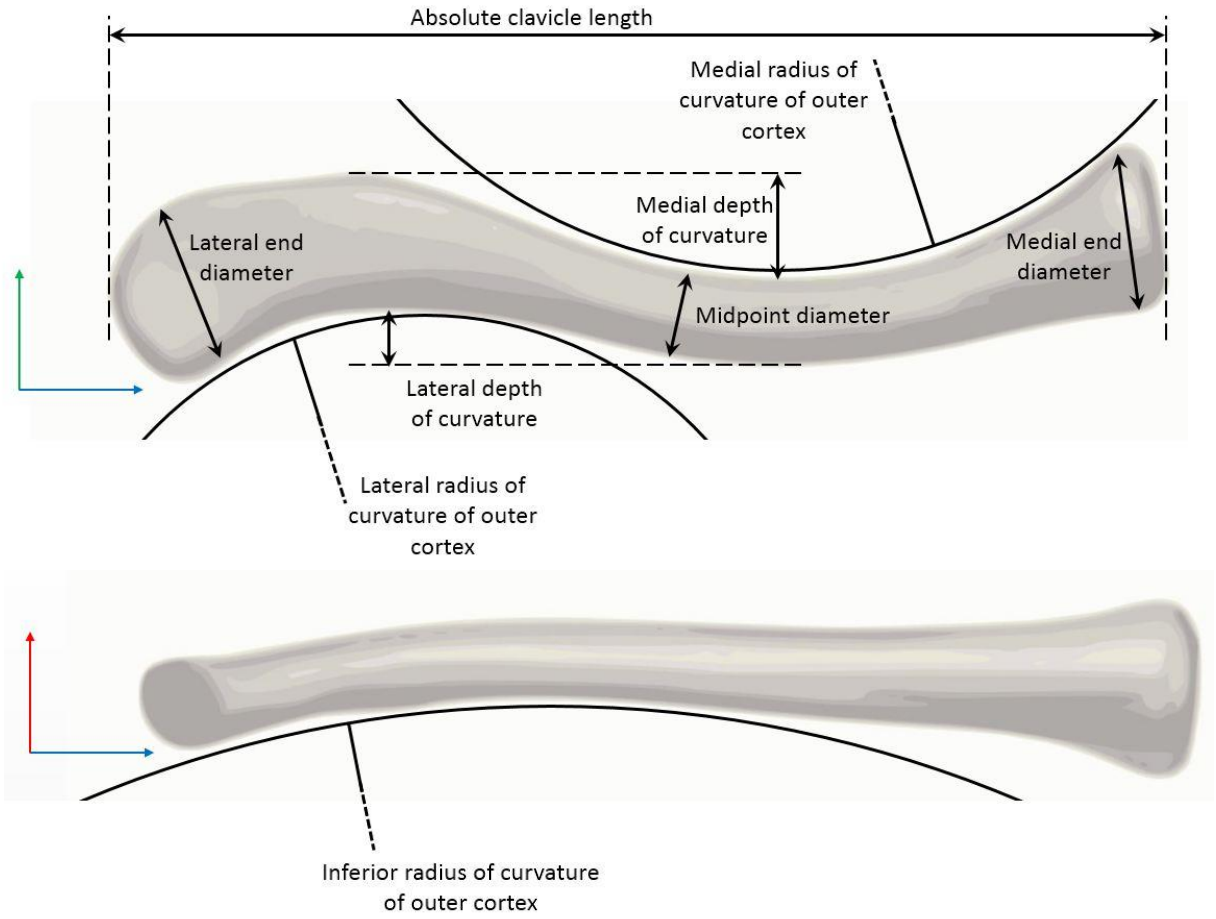

Figure A.2 Additional clavicle parameters

All the clavicle locations displayed are those the authors chose to report. The clavicle locations reported in previous studies have been approximated to their corresponding percentage of clavicle length in order to be comparable to the current study results. Refer to Figure A.1 for a description of the measurements taken.

Table A.1 Clavicle diameter (mm) compared to previous studies.

Clavicle Diameter	Clavicle Location	Grouping		King PR [7] *	Mathieu PA [5]	Bachoura A (2013) [10]****	Bachoura A (2012) [43] ****	Andermahr J [8]	Duprey S [14]	Daruwalla Z (Clin Anat) [13] *	Daruwalla Z (JOSR) [12] ***	Current Study
Clavicle Diameter	10%	Female	All							15.5 x 19.62	17.16	22.86
			Right							16.72 x 19.54		23.61
			Left							14.55 x 19.68		22.18
		Male	All							18.15 x 19.1	19.24	26.57
			Right							17.33 x 19.28		27.09
			Left							18.64 x 18.98		25.93
		Right								16.9 x 19.46		25.45
		Left								16.01 x 19.43		23.87
	17%	Female		12.27 x 13.57								17.51
		Male		14.55 x 14.55								21.52
	20%	Female	All							10.04 x 14.21		16.15
			Right							10.35 x 14.29		16.70
			Left							9.8 x 14.15		15.65
		Male	All							14.63 x 15.87		20.05
			Right							13.13 x 14.47		20.39
			Left							15.83 x 17		19.64
		Right								11.28 x 14.35		18.65
		Left								11.81 x 15.1		17.45
	30%	Female	All							9.44 x 11.3		13.33
			Right							9.44 x 11.44		13.91
			Left							9.44 x 11.19		12.82
		Male	All							13.5 x 14.4		16.73
			Right							12.34 x 14.02		17.12
			Left							14.43 x 14.71		16.25
		Right								10.4 x 12.3		15.60
		Left								11.1 x 12.36		14.37
	40%	All					12.4					14.01
		Female	All							9.64 x 9.9		12.31
			Right							9.58 x 10.03		12.71
			Left							9.68 x 9.8		11.96
		Male	All							13.16 x 12.78		15.77
			Right							12.22 x 13.02		16.21
			Left							13.92 x 12.59		15.24
		Right								10.46 x 11.03		14.56
		Left								11.1 x 10.73		13.44
	50%	All				10.9		12	11			13.75
		Female	All	11.08 x 9.36	9.9			11		9.59 x 9.34	9.18	12.01
			Right							9.56 x 9.45		12.29
			Left							9.62 x 9.26		11.76
		Male	All	12.71 x 10.97	12			13		12.78 x 11.69	12.12	15.57
			Right							12.05 x 12.11		15.74
			Left							13.36 x 11.35		15.36
		Right			11.1			12		10.39 x 10.34		14.11
		Left			10.8			12		10.86 x 9.96		13.38

Table A.1 (Continued)

Parameter	Clavicle Location	Grouping		King PR [7] *	Mathieu PA [5]	Bachoura A (2013) [10]****	Bachoura A (2012) [43] ****	Andermahr J [8]	Duprey S [14]	Daruwalla Z (Clin Anat) [13] *	Daruwalla Z (JOSR) [12] ***	Current Study
Clavicle Diameter	60%	Female	All							11.35 x 9.27		13.11
			Right							11.16 x 9.5		13.34
			Left							11.5 x 9.08		12.91
		Male	All							14.21 x 11.21		16.71
			Right							13.57 x 11.85		17.09
			Left							14.72 x 10.71		16.24
		Right								11.96 x 10.28		15.32
		Left								12.57 x 9.62		14.41
	70%	Female	All							14.71 x 9.71		16.58
			Right							14.48 x 9.97		16.83
			Left							14.9 x 9.51		16.36
		Male	All							18.44 x 11.58		19.11
			Right							17.61 x 11.94		19.69
			Left							19.1 x 11.3		18.40
		Right								15.52 10.63		18.34
		Left								16.3 x 10.1		17.28
	80%	All					14.9					20.17
		Female	All							15.08 x 9.64		18.67
			Right							14.71 x 9.64		19.26
			Left							15.37 x 9.64		18.14
		Male	All							19.05 x 11.03		21.72
			Right							17.83 x 10.76		22.53
			Left							20.02 x 11.25		20.75
		Right								15.75 x 10.01		20.99
		Left								16.92 x 10.18		19.31
	83%	Male		18.26 x 10.56								22.90
		Female		15.14 x 9.74								19.38
	90%	Female	All							20.01 x 9.72	14.73	24.40
			Right							19.49 x 10.06		24.94
			Left							20.43 x 9.44		23.92
		Male	All							24.59 x 11.41	18.37	29.76
			Right							26.77 x 11.49		29.76
			Left							22.84 x 11.34		29.75
		Right								21.91 x 10.54		27.49
		Left								21.24 x 10.08		26.55

* Measurements taken as Width x Height
** Measurements taken as Anteroposterior x Superoinferior
*** Multiple measurements averaged
**** Largest measurment from cross-section

Table A.2 Location (%) and value (mm) of the maximum clavicle diameter reported by previous studies.

Parameter	Clavicle Section	Grouping	Width/Height	Bernat A [9]		Current Study	
				Diameter	Location (%)	Diameter	Location (%)
Location and Value of Max. Clavicle Diameter	Medial	All	W	23.8	4.8%	29.09	5%
			H	25.6	4.9%		
		Female	W	22.8	4.6%	27.18	5%
			H	25.4	5.0%		
		Male	W	24.7	5.0%	31.07	5%
			H	25.7	4.8%		
		Right	W	24.3	5.0%	29.38	6%
			H	25.6	5.0%		
		Left	W	23.2	4.7%	28.88	5%
			H	25.5	4.8%		
	Lateral	All	W	24.7	91.4%	27.32	92%
			H	13.6	84.6%		
		Female	W	23.5	91.9%	24.81	92%
			H	12.7	86.2%		
		Male	W	25.9	90.8%	30.05	91%
			H	14.6	83.0%		
		Right	W	24.8	91.5%	27.80	91%
			H	13.9	83.0%		
		Left	W	24.7	91.3%	27.07	92%
			H	13.4	86.2%		
Location and Value of Min. Clavicle Diameter	All		W	10.9	38.4%	13.73	49%
			H	9.5	71.5%		
	Female		W	9.8	39.9%	11.98	49%
			H	8.7	71.1%		
	Male		W	11.9	37.0%	15.53	46%
			H	10.2	71.9%		
	Right		W	10.9	39.5%	14.11	48%
			H	9.4	69.4%		
	Left		W	10.8	37.4%	13.43	41%
			H	9.5	73.6%		

Table A.3 IM Canal diameter (mm) compared to previous studies

Parameter	Clavicle Location	Grouping	King PR [7] *	Mathieu PA [5] **	Andermahr J [8] ***	Current Study
IM Canal Diameter	15%	All			18	10.05
		Female		14.3 x 16.1		8.82
		Male		21.2 x 17.6		11.34
		Right		18.2 x 16.6		10.60
		Left		17.3 x 17.1		9.48
	17%	Female	8.12 x 8.88			7.89
		Male	10.24 x 9.82			10.40
	25%	All			11	6.82
		Female		12.3 x 10.9		5.67
		Male		15.6 x 13.7		8.02
		Right		14.3 x 12.7		7.21
		Left		13.6 x 11.9		6.41
	33%	All			8	5.60
		Female		4.1 x 3.3		4.71
		Male		8 x 6.8		6.53
		Right		6.4 x 5.3		5.89
		Left		5.7 x 4.8		5.30
	50%	All			6.7	4.53
		Female	5.97 x 5.00	2 x 1.9		3.86
		Male	7.34 x 6.26	3.1 x 3.1		5.22
		Right		2.7 x 2.6		4.78
		Left		2.4 x 2.4		4.26
	66%	All			7.5	5.52
		Female		3.7 x 2.9		4.93
		Male		6.1 x 5		6.14
		Right		5.1 x 4.1		5.85
		Left		4.7 x 3.8		5.18
	75%	All			12	6.19
		Female		10 x 7.2		5.48
		Male		11.9 x 9.1		6.94
		Right		10.8 x 8.4		6.77
		Left		11.1 x 7.9		5.60
	83%	Female	10.49 x 5.62			6.03
		Male	13.47 x 6.23			7.45
	85%	All			15	6.96
		Female		15.6 x 8.9		6.16
		Male		18.4 x 11.3		7.79
		Right		17.3 x 10.5		7.36
		Left		16.7 x 9.7		6.54

* Measurements taken as Width x Height
** Measurements taken as Anteroposterior x Superoinferior
*** Multiple measurements averaged
**** Largest measurment from cross-section

Table A.4 Radius of curvature of the clavicle outer surface compared to the IM canal. Note: no other studies have measured the radius of curvature of the IM canal.

Radius of Curvature of the Clavicle Outer Surface						Radius of Curvature of the IM Canal
Clavicle Section	Grouping	Mathieu PA [5]	Bachoura A (2013) [10]	Andermahr J [8]	Duprey S [14]	Current Study
Medial	All		66.4	71	62	91.21
	Female	68.7		70		87.58
	Male	72.1		73		94.99
	Right	70.7		69		88.86
	Left	70.1		74		93.67
Lateral	All		33.5	39	28	32.51
	Female	37.8		42		33.29
	Male	37.1		36		31.69
	Right	17.2		42		31.68
	Left	16.3		37		33.37

Table A.5 True and absolute clavicle lengths compared to previous studies

Parameter			King PR [7]	Mathieu PA [5]	Bernat A [9]	Bachoura A 2013 [10]	Bachoura A 2012 [43]	Andermahr J [8]	Duprey S [14]	Daruwalla Z (Clin Anat) [13]	Daruwalla Z (JOSR) [12]	Current Study
True Clavicle Length	All		151.15		159.0							166.62
	Right				158.0							165.87
	Left				159.8							167.41
	Female	All	145.79		151.0							158.07
		Right			150.4							157.24
		Left			151.7							158.81
	Male	All	156.87		166.8							175.51
		Right			165.7							173.56
		Left			167.8							177.88
Absolute Clavicle Length	All				149.4	136.7	136.0	151	147			151.76
	Right			147.1	148.4			149		143.24		150.59
	Left			145.8	150.3			152		145.21		152.98
	Female	All		140.2	142.9			146		140.34	142.17	143.86
		Right			142.3					133.27		142.53
		Left			143.5					141.1		145.05
	Male	All		152.7	155.8			156		152.33	152.87	159.97
		Right			154.6					151.19		157.78
		Left			157.0					153.2		162.64

APPENDIX B: SAMPLE CODE

```
folDir='\\Client\Q$\Personal Folders\Jazmine\Clavicles\';
cd(folDir);
d = dir(folDir);                                        % start with folder containing all subject subfolders
isub = [d(:).isdir];                                    % returns logical vector
IDFoldsimp = {d(isub).ID}';                             % creates cell with all names from structure
IDFoldsimp(ismember(IDFoldsimp,{'.','..'})) = [];       % removes folder names with . and ..
n = numel(IDFoldsimp);                                  % establish  amount of subjects

for f = 1:n;                                            % go through each subject
    fIDimport = IDFoldsimp{f,1};                        % make current subject ID a variable
    combpath = sprintf('%s%s', folDir, fIDimport);      % create entire path, specific to current patient
    cd(combpath);                                       % make it current folder
    disp(fIDimport);                                    % to view what subject we are on


     load 'canalHU.txt';
     load 'canalPC.txt';
     load 'clavicleHU.txt';
     load 'claviclePC.txt' ;
     load 'outerHU.txt';
     load 'outerPC.txt';

    side = fileread('side.txt');

    save(fIDimport, 'neckPoints', 'canal1PC', 'canalHU.txt',...
        'canalPC.txt', 'clavicleHU.txt', 'claviclePC.txt',...
        'outerHU.txt', 'outerPC.txt' );                 % save all variables as .mat to use later if re-run
%-------------------------------------------------------------------------------------------------------------------

    COORDnoPrompts                                      % scripts that do calculations on clavicles
    OUTERshapeALTjune
    INNERshapeALTjune
    clavCURV
    clavLENGTH

%-------------------------------------------------------------------------------------------------------------------
    prompt = '\n Continue? (y/n)\n';                    % verify code worked properly for each step by examining
                                                        % plots and figures from scripts
    str2 = input(prompt,'s');
    if str2 == 'y'
    clear str2;
    close all;
    save('Allvars', '-regexp',...
        '^(?!(|IDFoldsimp|f|n|folDir|str2)$).')         % save all variables except those pertinent to this loop

    clearvars -except fIDimport IDFoldsimp f n folDir   % clear all vars except those pertinent to loop
    end

end
```

Figure B.1 Sample code for the automated process described in methodology.

```
%% Allignment of clavicle and setting coordinate system that detects side of clavicle given txt file input

% PCA (applied to the volumetric model of clavicleHU)
% model must be perfectly filled

eigens=pca(clavicleHU(:,1:3));
p1=(eigens(:,1));
p2=(eigens(:,2));
p3=(eigens(:,3));

center=mean(clavicleHU(:,1:3));

l1=createLine3d(center,p1(1,1),p1(2,1),p1(3,1));
l2=createLine3d(center,p2(1,1),p2(2,1),p2(3,1));
l3=createLine3d(center,p3(1,1),p3(2,1),p3(3,1));

% model transformation (global to local)

i=p3';    % original global coordinates for clavicle
j=p2';
k=p1';

ii=[1 0 0];     % local
jj=[0 1 0];
kk=[0 0 1];

rotM=[i*ii' i*jj' i*kk';j*ii' j*jj' j*kk'; k*ii' k*jj' k*kk'];

% takes care of translations
clavicleHUZeroed=[clavicleHU(:,1)-center(1,1) clavicleHU(:,2)-center(1,2) clavicleHU(:,3)-center(1,3)];
claviclePCZeroed=[claviclePC(:,1)-center(1,1) claviclePC(:,2)-center(1,2) claviclePC(:,3)-center(1,3)];
outerHUZeroed=[outerHU(:,1)-center(1,1) outerHU(:,2)-center(1,2) outerHU(:,3)-center(1,3)];
outerPCZeroed=[outerPC(:,1)-center(1,1) outerPC(:,2)-center(1,2) outerPC(:,3)-center(1,3)];
canalHUZeroed=[canalHU(:,1)-center(1,1) canalHU(:,2)-center(1,2) canalHU(:,3)-center(1,3)];
canalPCZeroed=[canalPC(:,1)-center(1,1) canalPC(:,2)-center(1,2) canalPC(:,3)-center(1,3)];

% calculate rotations
transCLAV2=rotM*clavicleHUZeroed';
transCLAV=transCLAV2';

transCLAVpc2=rotM*claviclePCZeroed';
transCLAVpc=transCLAVpc2';

transOUThu2=rotM*outerHUZeroed';
transOUThu=transOUThu2';
transOUThu=[transOUThu,outerHU(:,4)];

transOUTpc2=rotM*outerPCZeroed';
transOUTpc=transOUTpc2';

transCANhu2=rotM*canalHUZeroed';
transCANhu=transCANhu2';

transCANpc2=rotM*canalPCZeroed';
transCANpc=transCANpc2';
```

Figure B.2 Code for establishing new coordinate system and creating plots

```
%% invert z-axis for left-sided clavicles only

if side == 'L'
    prompt = '\n Left sided clavicle\n';
    transCLAV(:,3) = transCLAV(:,3)*(-1);
    transCLAVpc(:,3) = transCLAVpc(:,3)*(-1);
    transCANhu(:,3) = transCANhu(:,3)*(-1);
    transCANpc(:,3) = transCANpc(:,3)*(-1);
    transOUThu(:,3) = transOUThu(:,3)*(-1);
    transOUTpc(:,3) = transOUTpc(:,3)*(-1);
else
    prompt = '\n Right sided clavicle\n';
end


% fitting box
clavicleBOX = boundingBox3d(transCLAV);


%% plots for clavicle

% original clavicle
% drawPoint3d(clavicleHU(:,1:3));
hold on
axis equal
axis auto
view([90 0])

drawLine3d(l1);
drawLine3d(l2);
drawLine3d(l3);
drawPoint3d(center);

% transformed clavicle
drawPoint3d(transCLAV);
drawBox3d(clavicleBOX);

% planes
drawPlane3d(planeBot);
drawPlane3d(planeTop);
drawPlane3d(planez12);
drawPlane3d(planez15);
drawPlane3d(planez45);

alpha(0.25)

% to plot transformed axis
hold on
drawPoint3d(transCLAV);
axis equal
axis auto
plot3([-30;30], [0;0],[0;0])
plot3([0;0], [-30;30],[0;0])
plot3([0;0], [0;0],[-85;80])

% to plot all planes that create slices
sliceplanes=zeros(100,9);
for s=1:100;
topslice=62.9623-(s-1)*thickness;
sliceplanes(s,1:9)=[0 0 topslice 0 1 0 -1 0 0];
drawPlane3d(sliceplanes(s,1:9));
alpha (0.25)
end
```

Figure B.2 (Continued)

APPENDIX C: TABLE OF TERMINOLOGY

Table C.1 Table of terminology used in the methods of the current study (chapter 3)

$[x_G,y_G,z_G]$	Global coordinate system
$[y_Gz_G]$	Global transverse plane
$[x_Gz_G]$	Global coronal plane
$[x_L,y_L,z_L]$	Local coordinate system
$[x,y,z]$	Principal directions
$C=[0,0,0]$	Geometric center
L_x	Horizontal height of the bounding box
L_y	Horizontal depth of the bounding box
L_z	Vertical length of the bounding box
$p_{(K)}$, $p_{(K+1)}$	A pair of consecutive planes p
r_c	Circumscribed radius
$C_c = [x_{Cc}, y_{Cc}, z_{Cc}\ (\text{func}\ (L_z)_{Cc})]$	Circumscribed circle center
r_i	Inscribed radius
$C_i = [x_{Ci}, y_{Ci}, z_{Ci}(\text{func}\ (L_z)_{Ci})]$	Inscribed circle center
CL_i	Centerline created by inscribed circle centers
CL_c	Centerline created by circumscribed circle centers